

Mangrove Encroachment into Ecologically Restored Salt Marshes: Quantifying
Vegetative and Soil Carbon in Tampa Bay, Florida

by

Emma E. Dontis

A thesis submitted in partial fulfillment
of the requirements for the degree of
Master of Science
Department of Environmental Science and Policy
College of Arts and Sciences
University of South Florida St. Petersburg

Major Professors: Christopher F. Meindl, Ph.D.
Ryan P. Moyer, Ph.D.
Kara R. Radabaugh, Ph.D.
James E. Ivey, Ph.D.

Date of Approval:
June 29, 2018

Keywords: Coastal wetlands, Blue carbon, Carbon credits, Climate change, Tampa Bay

Copyright © 2018, Emma E. Dontis

DEDICATION

I dedicate this thesis to my parents, Ernie and Jenni Dontis, for always supporting my endeavors (and financing many of them!).

ACKNOWLEDGEMENTS

I would like to thank my thesis advisor, Chris Meindl, as well as my committee members, Ryan Moyer, Kara Radabaugh, and Jim Ivey, for their guidance and supervision through this process. I am grateful to Pinellas County, Hillsborough County, Manatee County, the Southwest Florida Water Management District, and Florida State Parks for granting land access. I am thankful for Kent Smith (Fish and Wildlife Research Institute) for providing the funding for this project, and Brandt Henningsen, Mary Barnwell, Michael Elswick, and Karen Schanzle for providing land access. Ryan Moyer and Kara Radabaugh (Fish and Wildlife Research Institute) deserve additional thanks for providing laboratory access and assisting me with data analysis. I would also like to thank the following for their help with lab and field work: Kara Radabaugh, Ryan Moyer, Amanda Chappel, Josh Breithaupt, Sierra Greene, Christine Russo, Reba Campbell, Taylor Nielsen, Dana Parkinson, Victoria Manzella, Stuart Penoff, Ioana Bociu, Brad Furman, Ashley Huber, Regi Rodriguez, Sam Bathon, and Natasha Méndez-Ferrer. Finally, special thanks goes to Amanda Chappel for keeping me sane through this whole process!

TABLE OF CONTENTS

List of Tables	vi
List of Figures	vii
Abstract	ix
Introduction.....	1
Coastal Wetlands	1
Blue Carbon	4
Ecological Restoration	5
Carbon Credits	7
Mangrove Encroachment	8
Hypotheses	10
Methods.....	13
Tampa Bay	13
Site Selection	13
Remote Imagery	14
Sampling Design.....	14
Biotic Factors	15
Abiotic Factors.....	18
Data Analysis	20
Results.....	21
Remote Imagery	21
Biotic Factors	21
Carbon Storage.....	23
Abiotic Factors.....	24
Comparison to Natural Sites	24
Discussion.....	26
Analysis of Sampling Techniques	26
Site Vulnerability to Mangrove Encroachment	28
Impacts of Mangrove Encroachment	32
Carbon Storage.....	34
Carbon Sequestration	37
Comparison to Natural Sites	38
Conclusion	42

Tables	44
Figures.....	48
References.....	65
Appendix A: Supplemental Abiotic Figures.....	76

LIST OF TABLES

Table 1. Mangrove encroachment rates into salt marsh restoration sites	44
Table 2. Novel allometric equations generated in this study	45
Table 3. Vegetative and soil organic carbon storage at each restoration site	46
Table 4. Comparison of organic carbon stocks in restored and natural salt marshes, transitional habitats, and mangroves.....	47

LIST OF FIGURES

Figure 1. Locations of the ten restored coastal wetlands in Tampa Bay that were examined in this study	48
Figure 2. Aerial imagery of the ten restoration sites in the past and near-present.....	52
Figure 3. Encroachment rate comparison	53
Figure 4. Vegetative percent cover compared to site age	54
Figure 5. Comparison of tree characteristics	55
Figure 6. Biomass comparison amongst young, middle-aged, and old sites	56
Figure 7. Comparison of vegetative biomass to site age	57
Figure 8. Total organic carbon storage across the ten restoration sites	58
Figure 9. Organic carbon storage across young, middle-aged, and old restoration sites	59
Figure 10. Average organic carbon storage plotted against site age to calculate the rate of carbon sequestration	60
Figure 11. Soil organic carbon storage Compared to total vegetative OC storage across the ten sites.....	61
Figure 12. Average soil and vegetative organic carbon storage compared to site age.....	62
Figure 13. Dry bulk density and soil organic carbon comparison	63
Figure 14. Comparison of site age and average percentage of sand and mud.	64

Figure A1. Depth to porewater compared to salinity in the wet season 2016, dry season 2017, and wet season 2017.....	76
Figure A2. Average open water dissolved oxygen percentage compared to average open water salinity across the ten sites.....	77
Figure A3. Site age compared to average pH of the top 5-cm of soil.....	78
Figure A4. Seasonal comparison of average soil pH, depth to porewater, and porewater salinity.....	79
Figure A5. Seasonal comparison of average open water dissolved oxygen percentage and open water salinity.....	80

ABSTRACT

Coastal wetlands are one of the world's most productive and valuable ecosystems. Mangrove forests, salt marshes, and salt barrens are the dominant coastal wetlands in the Tampa Bay estuary. These "blue carbon" sinks absorb carbon dioxide and store organic carbon (OC) in their vegetation and underlying sediments, allowing them to partially mitigate climate change. However, the global areal extent of these ecosystems has declined by 25-50 %, so restoring critical coastal wetland habitats has become imperative. Created coastal wetlands in the Tampa Bay area are first planted with salt marsh vegetation, but often transition into mangrove forests, a process known as mangrove encroachment. This study investigated the rates of mangrove encroachment and hypothesized that middle-aged (6- to 13-year-old) restoration sites would experience the fastest rate of mangrove encroachment. The rate of encroachment was determined through remote imagery, while biomass calculations via allometry, point-center-quarter (PCQ) analysis, and percent cover estimations provided supplemental ground-truthing. The average encroachment rate among all sites was 0.62 m y^{-1} , but no difference was found between the encroachment rate at old (14- to 27-year-old) and middle-aged restoration sites, and no trees were observed at young sites (< 5 years old). The second aim of this study was to calculate a total carbon stock for each site. It was hypothesized that old restoration sites would store the most OC. This hypothesis was investigated by calculating carbon stocks with the use of allometric calculations, PCQ analysis, and soil core analyses. Indeed, mature mangrove-dominated

restoration sites had higher total carbon stocks ($138.7 \pm 13.8 \text{ Mg C ha}^{-1}$) than middle-aged transitional sites ($85.6 \pm 25.5 \text{ Mg C ha}^{-1}$) or young salt marshes ($34.5 \pm 7.7 \text{ Mg C ha}^{-1}$). A comparison of these calculated carbon stocks to natural coastal wetlands in Tampa Bay and the eastern coast of Florida demonstrated that there was no difference in OC storage between natural and restored sites. The carbon sequestration rate across the 26-year chronosequence was found to be $4.68 \text{ Mg C ha}^{-1} \text{ y}^{-1}$. This value is higher than calculated values in other Florida studies, as it considers both vegetative and soil OC. The quantification of total carbon storage over time may incentivize coastal managers to pursue blue carbon restoration projects, because such projects store large quantities of carbon, and can generate carbon credits that can be sold to generate more revenue for additional coastal restoration projects.

Introduction

Coastal Wetlands

Coastal wetlands are one of the world's most productive and valuable coastal ecosystems, providing ecosystem services such as coastal protection, erosion prevention, and nutrient cycling. They also act as sinks for sediments, sites for carbon sequestration, and provide nursery grounds for fisheries (Crossland et al. 2005; Kirwan and Megonigal 2013; Osland et al. 2013; Doughty et al. 2015). They serve as zones of transition between terrestrial and marine ecosystems, usually containing rich organic soil that is covered or saturated with tidal brackish waters (Kennedy et al. 2013). Along Florida's coastal zone, coastal wetlands include a diverse array of intertidal marshes, mangrove swamps, mud flats, seagrass beds, hypersaline lagoons, and salt barrens (Michener et al. 1997).

Despite the benefits coastal wetlands provide, globally mangroves have been lost at a rate of 0.7-3 % annually since the 1940s and salt marshes have been lost at a rate of 1-2 % each year since the 1800s, with total losses estimated to be 25-50 % (McLeod et al. 2011; Kirwan and Megonigal 2013). This is largely because they are being converted into land for agriculture, aquaculture, and urban development (Donato et al. 2011; Michener et al. 1997; McLeod et al. 2011; Kirwan and Megonigal 2013). In other cases, wetlands are converted into open water, largely attributed to strong coastal storms that cause storm surges, increased rainfall, and abnormally high tides (Dahl and Stedman 2013). Other indirect anthropogenic impacts to coastal wetlands include: restructuring of the landscape, urban development and agriculture, chemical contamination, overharvesting of

fish/shellfish, and heightened sediment inputs, which result in a loss of habitat and biodiversity, eutrophication, and erosion (Crossland et al. 2005). Additionally, horizontal or inland advancement of salt/brackish water, a consequence of sea-level rise (SLR) and altered hydrology, could significantly alter coastal habitats, potentially harming wetland-dependent species. An estimated 90 % of important recreational and commercial fish and shellfish species spend some of their life cycle in seagrass meadows, salt marshes, or mangroves, all of which may be harmed by rising seas and corresponding loss of habitat (Glick and Clough 2006).

Mangrove and salt marsh ecosystems have long lined the coast of the Tampa Bay Estuary. In the 1950s, Tampa Bay featured roughly 9,700 ha of salt marshes (28 %), salt barrens (6 %), and mangrove forests (66 %) combined (Robison et al. 2010). It is estimated that Tampa Bay lost 21 % (nearly 2,000 ha) of its tidal wetland habitats from 1950 to 1990, largely a consequence of development activity. Indeed, most of the tidal wetlands around Tampa Bay were ditched in an effort to eradicate the salt marsh mosquito *Aedes taeniorynchus*; however, this leads to habitat degradation (Smith et al. 2007). Today, there are an estimated 8,100 to 8,300 ha of remaining and restored coastal wetland habitat in the Tampa Bay Estuary (Robison et al. 2010; SWFWMD 2012).

Coastal wetlands can play a role in the carbon cycle. Mangroves are salt-tolerant, frost-intolerant trees found along subtropical and tropical coastlines that are extremely rich in carbon, a result of high primary productivity and the slow rate of microbial decomposition, a consequence of frequent inundation and anaerobic soils (Osland et al. 2012). The carbon dioxide (CO₂) that mangroves extract from the atmosphere is used to manufacture new roots, leaves, and branches, maintain existing stem tissue, and develop

chemical defenses against herbivory (Alongi 2014). Beneath the mangroves, carbon accumulates in thick layers of peat (a mixture of fresh and decaying organic matter (OM)). In mangrove forests, the greatest carbon pool is in the soil, which comprises of 75 % of the total OC within the system, while live and dead vegetation accounts for 25 % of the carbon stock (Alongi 2014). On an area-specific basis, mangroves store more carbon than any other ecosystem. They only make up 0.5% of the global coastal area, as they only exist in tropical and sub-tropical regions, yet contribute 10-15 % of coastal sediment carbon storage (Alongi 2014).

Salt marshes are characterized by salt-tolerant herbaceous plants and low shrubs and have greater latitudinal distribution than mangroves (Kennish 2001). Accretion, the vertical building of soils by the deposition of mineral sediment and OM, is accelerated by salt marsh presence because the vegetation provides a substrate for OM and sediment to adhere to, which also decreases erosion (Kennish 2001). Belowground biomass has proven to be critical in the long-term survival of salt marshes. It contributes to the volume and thus, elevation, of the marsh, which Darby and Turner (2008) speculate as being more important than inorganic matter for a salt marsh to maintain itself. Like mangrove forests, soil OM is the largest carbon pool in salt marshes and contains 90 % of total OC in the system (Alongi 2014).

Salt barrens, a third wetland type occurring in the Tampa Bay Estuary, are hypersaline (soil salinity above 35) flats located in the upper intertidal zone that are inundated only by spring high tides (Lewis and Robison 1995). They are typically located further inland than mangrove forests or salt marshes at slightly higher elevations. Salt barrens experience seasonal expansion of salt-tolerant vegetation in the rainy season and

retreat in the dry season when salts concentrate the soil (Lewis and Robison 1995). The largest OC pool in salt barrens is the soil, although total OC is much lower than that of mangroves and salt marshes (Radabaugh et al. 2018).

Blue Carbon

“Blue carbon” refers to carbon that is stored in coastal and marine ecosystems. Mangroves, salt marshes, and seagrasses are the prominent vegetated blue carbon sinks. They receive carbon from both allochthonous (material produced elsewhere – seagrass, algae, drift wood, sediment etc.) and autochthonous (produced in situ by the uptake of CO₂ by plants to create leaves, roots, stems, etc.) sources (Howard et al. 2014). Coastal vegetated ecosystems experience high sedimentation, driven by tidal inundation and storm-surge events, which bring in allochthonous organic and mineral material, referred to as particle accretion (Nyman et al. 2006; Smith et al. 2009; Breithaupt et al. 2017). Together, particle accretion and expansion, which occurs when belowground roots grow and expand, cause the land elevation to rise (Castañeda-Moya et al. 2010; Breithaupt et al. 2017). The accretion of sediments in coastal zones is an example of a positive feedback mechanism in which coastal wetlands are able to maintain their position in the intertidal zone in response to sea-level fluctuations.

A carbon stock refers to the amount of OC stored in a blue carbon ecosystem up to a specific depth. Carbon stocks are determined by adding up the carbon pools within the system (Howard et al. 2014). The relevant pools of blue carbon systems are: underlying sediments, aboveground living biomass (leaves, stems, branches), belowground living biomass (roots and rhizomes), and non-living biomass (leaf litter and dead wood) (McLeod et al. 2011). Carbon stored in biomass can exist for years to decades, whereas carbon

sequestered in sediment can be stored for thousands of years if undisturbed (McLeod et al. 2011). Across all three blue carbon sinks, soil carbon is the dominant carbon pool (Howard et al. 2014). Mangrove forests also have significant aboveground living and dead biomass, unlike herbaceous blue carbon ecosystems such as salt marshes and seagrass beds, which lack large vegetation. Global averages for whole-ecosystem carbon stock estimates are: 956 metric tons of carbon per hectare ($t\ C\ ha^{-1}$) for mangroves, 593 $t\ C\ ha^{-1}$ for salt marshes, and 142 $t\ C\ ha^{-1}$ for seagrasses (Alongi 2014).

Through photosynthesis, vegetated blue carbon sinks absorb and convert CO_2 into OM, and can partially mitigate climate change (Howard et al. 2014). But, to mitigate anthropogenic CO_2 emissions, the magnitude of the carbon sink must increase over time. This can be achieved by increasing the areal extent of blue carbon systems and increasing the total rate of carbon sequestration (Hopkinson et al. 2012); however, unless the annual rate of global CO_2 emissions decreases, the amount of carbon sequestered by these ecosystems will be miniscule compared to emissions (Alongi 2014). Nevertheless, coastal wetland restoration and preservation projects remain attractive to climate change mitigation programs. These natural ecosystems are an efficient, cost-effective approach to offsetting greenhouse gas (GHG) emissions from companies or small regions (Villa and Bernal 2017).

Ecological Restoration

Ecological restoration refers to a process in which a destroyed, damaged, or degraded ecosystem is recovered (SER 2002), and is often necessary when an ecosystem has been altered to the point where it cannot self-correct or self-renew, secondary succession and natural recovery from damage is inhibited, and ecosystem homeostasis

stops (Lewis 2005). The two main goals of ecological restoration are to: 1) restore ecosystems that have been disturbed by humans, and 2) develop new sustainable ecosystems that have economic and ecological value (Lewis 2005). For the purposes of this study, only sites that were created with these two goals in mind were characterized as ecological restoration sites. Salt marsh restoration sites are attempts to recreate naturally occurring habitats and may help facilitate the regrowth of important salt marsh ecosystems, but they are not always perfect duplicates for natural salt marshes.

Ecological restoration can provide an opportunity for creating or enhancing habitats that provide ecosystem services that were previously lost to development or other anthropogenic impacts. Tidal salt marshes and salt barrens have experienced disproportionately greater losses than mangrove forests in the Tampa Bay area, currently accounting for 20 % of the region's coastal wetlands, so there have been ongoing efforts to restore these critical habitats (Lewis and Estevez 1988). Coastal wetlands are created from open-water areas by pumping dredge material onto them or from upland habitat by removing sediment until elevations are appropriate for tidal inundation (Edwards and Proffitt 2003). Next, flora that are tolerant to anoxic soil conditions and frequent saltwater flooding are planted, such as *Spartina alterniflora* (smooth cordgrass), which creates immediate structural habitat, stabilizes substrates, and accelerates secondary succession (Freiss et al. 2012; Osland et al. 2012). Mangroves are usually not planted at restoration sites in Tampa Bay because they can self-colonize. Mangroves have propagules (germinated 'seeds') which float with the tides and can be transported to new locations easily, while salt marsh species colonize by extending laterally through marsh sediment and via seed dispersal (Raabe et al. 2012). Salt marsh vegetation can also trap mangrove

propagules, facilitating mangrove colonization (Stevens et al. 2006). Ultimately, successful colonization depends on species fecundity, dispersal capacity, and appropriate hydrology and elevation (Freiss et al. 2012).

Tampa Bay Estuary Program's (TBEP) Habitat Master Plan, originally drafted in 1995, set restoration targets, defined by areal coverage, for mangroves, salt marshes, and salt barrens (Lewis and Robison 1995). In 2010, the Habitat Master Plan was updated to prioritize the "Restore the Balance" approach, which was designed to return coastal wetlands to historical (1950s) habitat ratios in the Tampa Bay Estuary (Robison et al. 2010). Because many organisms utilize different habitats at different life stages, restoring the balance of coastal wetland types may help prevent bottlenecks in the life history of Tampa Bay species by placing an emphasis on restoring habitats that have disproportionately been lost, such as salt marshes and salt barrens (Holland et al. 2006).

Carbon Credits

Because of their potential to offset CO₂ emissions, restoring and creating coastal wetlands has become a popular management tool to obtain carbon credits (DeLaune and White 2012). To begin a restoration project with the intention of earning carbon credits, coastal managers can follow the Verified Carbon Standard (VCS) Methodology for Tidal Wetlands and Seagrass Restoration protocol, which outlines the procedure to estimate net CO₂ reductions (VCS 2015). The methodology, facilitated by the national 501(c)(3) non-profit organization Restore America's Estuaries, covers project eligibility criteria to receive credits and accounting procedures within markets (VCS 2015; Sutton-Grier and Moore 2016). Coastal landowners can then sell or trade credits, which gives them an incentive to pursue mitigation and restoration projects. Although project managers may be in financial

deficit after completing the project, the carbon storage that coastal wetlands provide is highly valued in most carbon markets (Sutton-Grier and Moore 2016).

Under the Intergovernmental Panel on Climate Change (IPCC) guidelines, nations that have signed and ratified the Kyoto Protocol may trade excess carbon emissions for “carbon credits” (Villa and Bernal 2017). The Protocol established emissions standards for participating nations, and if they remain below their standard, they will receive tradeable allowances (Villa and Bernal 2017). One ton of CO₂ or GHG equivalent equates to one carbon credit, but the value of the credits themselves varies (DeLaune and White 2012). In the U.S., where only a voluntary market exists, a credit can range from \$1 to \$15 (DeLaune and White 2012). However, a lack of federal action has resulted in lowered carbon credit value, with a peak of \$30 per ton of CO₂ in 2008 and a lowest point of \$0.05 per ton in 2010 (Gardner and Fox 2013). Because there is no federally mandated cap-and-trade system in the U.S., the voluntary carbon market sets prices for carbon credits. At current prices, revenue generated from carbon credits may not be enough to offset the total cost of restoration projects (Sutton-Grier and Moore 2016). Nevertheless, the global carbon market is expanding, and increased from \$11 billion in 2005 to nearly \$142 billion in 2010 (Linacre et al. 2011).

Mangrove Encroachment

Since the 1960s, average air temperatures in Florida have risen 1.1 °C, and are projected to increase by another 1.65 to 3.85 °C by 2100 (Sherwood and Greening 2014). Mangroves thrive in tropical/sub-tropical climates, whereas salt marshes dominate coastal wetlands in temperate climates. The Tampa Bay estuary is uniquely situated at the extent of these ecosystem ranges and supports both mangrove and salt marsh habitats. During

freeze events, mangroves suffer mortality, lose their leaves, and expose the forest floor to sunlight, allowing some salt marsh vegetation to grow (Kangas and Lugo 1990; Stevens et al. 2006). However, Florida has experienced fewer cold days (defined as < -4 °C) in the winters and warmer average winter temperatures since 1970, which allows mangroves to expand northward beyond their historical range (Osland et al. 2013; Cavanaugh et al. 2014). Therefore, global warming is likely one of the factors driving the transition from salt marsh to mangrove forest in the Southeastern United States (Raabe et al. 2012; Osland et al. 2013).

A 1-m increase in eustatic sea level could threaten up to 70 % of the world's coastal wetlands (Friess et al. 2012). From 1993-2010, the rate of global SLR was about 3.2 ± 0.4 mm y^{-1} , and this rate is expected to accelerate (Church et al. 2013). In south Florida, it is predicted that SLR will range from 22.9 to 61.0 cm above 2010 levels by 2060, giving a rate of 4.6 to 12.2 mm y^{-1} (SFRCCC 2011; Breithaupt et al. 2017). These projected rates are higher than any observed long-term (≥ 50 years) rates on record and could result in a horizontal advance of water up to 76 m inland (Glick and Clough 2006; Breithaupt et al. 2017). Breithaupt et al. (2017) found the 10-year accretion rate of Florida mangroves to be 3.3 ± 0.5 mm y^{-1} , which is slightly lower than the global rate of SLR. Similarly, Gonneea (2016) calculated an average accretion rate of 2.8 ± 0.5 mm y^{-1} in Tampa Bay mangroves and salt marshes, thus many coastal ecosystems may be lost or forced to migrate inland. However, coastal wetlands may remain in place if they can accrete sediment at a rate equal to or exceeding the rate of SLR. Breithaupt et al. (2017) speculate that some sites in south Florida may be able to keep pace with SLR under a 4.6 mm y^{-1} scenario if the production and preservation of soil OM is sustainable over longer periods of time. If, however, the rate

of SLR reaches 12.2 mm y^{-1} , mangrove wetlands will need to receive annual deposition of 3.9 to $29.6 \text{ kg m}^{-2} \text{ y}^{-1}$ of sediment, equivalent to the mass deposited by Hurricane Wilma in south Florida (Castañeda-Moya et al. 2010; Breithaupt et al. 2017).

An increase in tidal flooding leads to more waterlogging in wetland soil, which stresses salt marsh vegetation and limits its primary production (DeLaune et al. 1994). Mangroves are more tolerant of tidal flooding and saline intrusion than salt marsh vegetation because of their unique root adaptations, which enable them to obtain oxygen from the atmosphere under anoxic conditions (Raabe et al. 2012). Some salt marsh species can survive prolonged inundation, such as *S. alterniflora*, which typically grows along the water's edge, but may be replaced as mangroves expand (Lewis and Robison 1995). Because of mangrove root modifications and tolerance of inundation, coastal wetlands in much of Florida often include a mangrove fringe along the water which then transitions to salt marshes further inland. Over the past 100 years, mangroves across Florida, including Tampa Bay, have encroached inland into salt marsh habitats as a result of SLR and altered surface water hydrology (Raabe et al. 2012; Krauss et al. 2017). Given current trends of natural mangrove recruitment into created and natural salt marsh and salt barren habitat, habitat balance has not been achieved in the Tampa Bay estuary (TBEP 2017).

Hypotheses

Given the importance of mangroves and salt marshes to the Tampa Bay estuary, this study seeks to gain further insight into how these ecosystems are changing. Its objectives are to: 1) assess and determine the rate of mangrove expansion into restored salt marsh sites throughout the Tampa Bay Estuary, and 2) model carbon storage across the restoration sites to develop simplified estimates of carbon stocks in transitioning

ecosystems. From here, two null hypotheses have been established: 1) there will be no difference in the rate of mangrove expansion at restoration sites of different ages, and 2) restoration sites will have similar vegetative and soil carbon stocks, regardless of age. Further, two hypotheses have been constructed: 1) middle-aged (6- to 13-year-old) restoration sites will experience the fastest rates of mangrove encroachment, and 2) mature salt marsh restoration sites will have greater vegetative and soil carbon stocks than recently restored sites.

By quantifying the rate of mangrove encroachment, ecological restoration sites that are capable of maintaining stable salt marsh habitat and sites that are vulnerable to mangrove encroachment in the Tampa Bay estuary can be determined. Mangrove encroachment is expected to continue in the Tampa Bay estuary, a consequence of both SLR and warmer winter temperatures, so the determination of rates of mangrove intrusion into restored salt marsh habitats helps to evaluate the feasibility of the “Restore the Balance” approach to managing Tampa Bay’s coastal habitats. More long-term research is needed to assess the success of restored and created sites in meeting their habitat ratio goals. Thus, the information obtained from this study will assist in evaluating the efficacy of future salt marsh restoration projects by determining if any sites deviate from the standard rate of encroachment and are therefore resistant to mangroves. This information may be valuable to coastal resource managers, as they seek to maximize the potential of future wetland mitigation efforts.

Further, this study will quantify carbon storage in restoration sites of varying ages. By quantifying the aboveground vegetation and belowground soil carbon pools of these restoration sites, simplified carbon stocks can be estimated. A comparison of carbon

storage across the 26-year chronosequence also enables calculation of the rate of carbon sequestration in restoration sites. Data collected in this study will support and facilitate further monitoring of restoration sites and increase awareness on the importance of coastal wetlands, especially their potential to partially reduce atmospheric CO₂ and ultimately lessen the effects of climate change. Little information was found on rates of carbon sequestration in coastal wetlands in Florida. Studies that were found (i.e. Breithaupt et al. 2014; Marchio et al. 2016) did not calculate aboveground OC, and no information was found on sequestration rates in restored wetlands, so this study will be of interest to potential carbon-credit investors.

Methods

Tampa Bay

Tampa Bay, Florida's largest open-water estuary, is located along the central Gulf of Mexico Coast, spanning Hillsborough, Pinellas, and Manatee Counties. It covers approximately 1,000 km² and has an average depth of 4 m, but can be as deep as 15 m in dredged channels (Chen et al. 2007). The bay receives freshwater runoff from the surrounding watershed, which encompasses around 5,700 km² (Yates and Greening 2011). The Tampa Bay region experiences a humid sub-tropical climate, characterized by periods of heavy rain in the summers (June-September) and mild, dry winters (October-May).

The Tampa Metropolitan Area is home to over three million people, an 8.9 % increase from 2010 to 2016 (U.S. Census Bureau 2017). This number is predicted to grow, putting increasing pressure on surrounding coastal areas. In 2007, scientists estimated that 42 % of the Tampa Bay watershed has been developed (Sherwood and Greening 2014), and further development will threaten Tampa Bay's critical coastal wetland ecosystems. Since the 1880s, parts of the Tampa Bay shoreline and bathymetry have been altered to cater to shipping and other economic needs (Yates and Greening 2011). Many freshwater inputs have also been dammed or impounded to provide people with freshwater.

Site Selection

Ten restored wetland sites were selected along the coastline of Tampa Bay (Fig. 1). Each site was originally planted with salt marsh vegetation between the years 1990 and

2016, spanning a range of 26 years (Table 1). All sites displayed typical coastal wetland vertical zonation patterns, with clear distinctions between each zone, along an elevation gradient from the water's edge to the transition to upland habitat. In most cases, lower elevations were dominated by an abundance of mangroves that extended from the water's edge to the adjacent high marsh. The high marsh zone was characterized by salt-marsh flora or salt barrens at all sites. Wet-season data collection began in July 2016 and concluded in September 2016. Dry-season sampling began approximately six months later, beginning in January 2017 and concluding in March 2017. Another round of wet-season data collection began in July 2017 and concluded in August 2017.

Remote Imagery

Satellite imagery from Google Earth version 7.1.8.3036 (Google Inc., Copyright © 2017) was used to estimate rates of mangrove encroachment. Images taken shortly after completion of the restoration (in most cases, see Table 1 and Fig. 2 for discrepancies) were compared to near-present-day images. Using these images and the digital path tool in Google Earth, the extent of mangrove fringe was measured along each transect to quantify inland expansion over time. Measurements began at the open-water shoreline and ended inland at a point where no mangroves were observed. To determine the encroachment rate, the measured distance was divided by the amount of time (in years) elapsed between aerial photographs.

Sampling Design

A shore-perpendicular, linear transect was established across the ecological zones at each site. Each transect began at the open-water's edge and extended upslope until upland vegetation was reached, and no more salt-tolerant vegetation was found. Total

transect lengths ranged from 8 to 68 m, as marsh widths and zonation patterns were site specific (Table 1). Six quadrat plots were placed within a 20-m-wide belt transect. The locations of the plots within this belt transect were determined with the use of a random number generator; however, it was ensured that at least one plot would fall within each zone of distinct vegetation. Each vegetative plot consisted of a 1 x 1-m quadrat, with a smaller 30 x 30-cm quadrat in the middle.

Biotic Factors

Vegetative canopy cover within the 1 x 1-m plot was visually estimated, referencing the National Estuarine Research Reserve System cover guide as needed (NERRS 2013). Total canopy cover was estimated for each plant species within and directly above the plot. Basal percent cover was also estimated for all flora within the plot. Within each 30 x 30-cm plot, heights of 25 stems of salt marsh species were measured to calculate plant biomass. For plants that were not present within the 30 x 30-cm plot, heights of 25 stems of each salt marsh species were measured within the 1 x 1-m plot. The total number of plants of each species within the plots was also recorded.

Mangroves were divided into three size classes: seedlings (< 30-cm tall), scrubs (30 to 130-cm tall), and trees (> 130-cm tall). In each 1 x 1-m plot, the number of seedlings was recorded, as were their corresponding heights. For scrubs, the number, height, canopy dimensions (crown length, width, and depth), and diameter at 30 cm (D_{30}) on the trunk were recorded. For trees, the species and diameter at breast height (DBH, 130 cm) were recorded. For any dead trees that fell within the plot, the decay status (1, 2, or 3) was determined, following the model of Howard et al. (2014). The DBH was measured for status 1 and 2 trees, while the diameter at the base and top of the trunk was recorded for

status 3 trees. The biomass of decay status 1 and 2 trees was found using the DBH and an average wood density of 0.431 g cm^{-3} (Radabaugh et al. 2018). For decay status 1 trees, 2.5 % of the biomass was subtracted from the total to account for loss of leaves (Howard et al. 2014). Similarly, 20 % of the total biomass was subtracted from the total for decay status 2 trees (Howard et al. 2014). Decay status 3 trees were identified by having few or no branches, and biomass was calculated from the tree's volume and wood density, assuming the tree was like a truncated cone (Howard et al. 2014).

Salt marsh aboveground biomass was calculated using allometric equations found in Radabaugh et al. (2017). For species of salt marsh vegetation without a known height-biomass relationship, plants were collected in the field, and placed into the refrigerator until ready for analysis. Howard et al. (2014) recommends collecting at least 50 individual stems, but this was not always feasible. In the laboratory, roots and rhizomes were cut from stems, and the total aboveground height was recorded to the nearest 0.1 cm. Stems were then put on trays and placed into an Isotemp 500 series or Heratherm OGS60 drying oven (Thermo Fisher Scientific, Waltham, MA) at $60 \text{ }^{\circ}\text{C}$ until a constant weight was reached (usually after 72 hours). Species-specific allometric biomass equations were then generated by creating linear regression models comparing dry mass to stem height. Regressions were analyzed with and without natural logarithmic transformations, and the final equation was chosen based on the graph that yielded the highest R^2 value.

Allometric equations used to calculate the aboveground biomass of living mangrove trees were obtained from Smith and Whelan (2006), mangrove scrub equations were from Ross et al. (2001), and mangrove seedling equations were from Ellison and Farnsworth (1997). Aboveground vegetative biomass (kg m^{-2}) was then calculated at each

site as a function of individual plant biomass and plant density. The DBH was used to calculate tree biomass using allometric equations. Equations to calculate aboveground biomass for *Conocarpus erectus* were found in Abohassan et al. (2010) and equations for *Baccharis halimifolia* and *Iva frutescens* were obtained from Appolone (2000). A general broadleaf equation was used for trees without species-specific allometric equations, which included *Schinus terebinthifolius* and *Caesalpinia bonduc* (Aguaron and McPherson 2012). Species-specific tree biomass and tree density from PCQ measurements were used to calculate aboveground vegetative biomass (kg m^{-2}) for trees at each site.

A secondary vegetation quantification method known as the point-centered-quarter (PCQ) method was utilized to estimate tree density, following the protocols of Cottam and Curtis (1956) and Mitchell (2015). Each quadrat was divided into four sub-plots (quarters), oriented parallel to the direction of the transect. The distance from the base of the tree nearest to the center of the 1 x 1-m plot was measured in each of the four quarters, as was the DBH and tree height. Because trees were not randomly distributed in the coastal habitat gradient, an equation for non-randomly spaced trees from Morisita (1957) was utilized to calculate tree density (trees ha^{-1}) and basal area coverage ($\text{cm}^2 \text{ha}^{-1}$). Rather than taking the average of all six plots, each plot was calculated separately, as suggested by Bouldin (2008), following the assumption that trees are more likely to be randomly distributed around each plot rather than across the entire site. Additionally, some plots did not have representative trees in all four quarters, so appropriate correction factors, derived by Warde and Petranka (1981), were applied.

To calculate the amount of OC stored in vegetative carbon pools, carbon conversion factors were multiplied by the plant biomass. For all mangrove and non-mangrove trees, a

carbon conversion factor of 0.44 was applied, as recommended by Ewe et al. (2006), Bouillon et al. (2008), and Radabaugh et al. (2017). The carbon content for all aboveground standing dead wood was assumed to be 50 %, or a conversion factor of 0.5 (Kauffman and Donato 2012; Howard et al. 2014). Carbon content for aboveground salt marsh vegetation was species-specific, utilizing carbon conversion values from Radabaugh et al. (2017). For species without a carbon conversion factor, the carbon content was assumed to be 41 % (Radabaugh et al. 2017). To find the carbon content of pneumatophores, a conversion factor of 0.39 was applied, as suggested by Kauffman and Donato (2012).

Abiotic Factors

At the water's edge, a YSI multi-parameter handheld meter (Yellow Springs Inc., Yellow Springs, OH) was used to measure water temperature (°C), optical dissolved oxygen concentration (mg L^{-1}) dissolved oxygen percent saturation (%), and salinity on the practical salinity scale. The probe was placed 10 to 20 cm below the water's surface. Depth to porewater (cm), porewater salinity, and soil pH were measured adjacent to each plot, so that the flora within the plot remained undisturbed. A hand auger was used to excavate a shallow hole for porewater collection. Porewater was measured using a Goldberg salinity refractometer (Reichert Technologies, Buffalo, NY), while depth to porewater was measured with a metric ruler, and soil pH was found using a Kelway soil pH meter (Kel Instruments Co., Wyckoff, NJ).

During both rounds of wet-season data collection, soil samples from the top 5 cm were taken from directly outside each 1 x 1-m plot for laboratory analysis of OC content and grain size. During the second round of data collection (dry season), cores ranging from 13 to 50 cm were obtained directly outside each of the plots at each site using a Russian-

style half cylinder peat corer (Eijkelkamp, Morrisville, NC). Until ready to be processed, cores and soil samples were kept in a refrigerator at 4.5 °C to prevent bacterial growth. To find the grain size of the soil samples, Fisherbrand USA standard test sieve shakers (Fisher Scientific International Inc., Pittsburgh, PA) were used, with mesh sizes ranging from 63 to 4,000 μm . The 5-cm samples were homogenized prior to sieving to ensure that the sample represented the entirety of the 5-cm interval. After shaking the sieves for 3-5 minutes, the weight of the soil on each sieve size was recorded to find the percentage of sand, gravel, and clay. Gravel was identified as sediment larger than 2 mm, while sand particles were between 0.0625 mm (63 μm) and 2 mm, and mud/clay were smaller than 0.0625 mm (63 μm) (Blott and Pye 2001).

To quantify the OC content, loss-on-ignition (LOI) analysis was performed (Craft et al. 1991). For the loose soil samples, the sample was homogenized by mixing the bag, and then a small portion of the soil was taken using a spatula. The soil cores were cut into 1-cm sections using a scalpel and a plastic cylinder was used to remove a cylindrical aliquot of known volume (1.131 cm^3) from each section. Aliquots from the loose soil samples and from the cores were placed into a weighed crucible, which were placed on ceramic trays. The trays were then put into a Thermolyne furnace (Thermo Fisher Scientific, Waltham, MA) and dried for 24 hours at 105 °C. After removing the crucibles and allowing them to cool down, the dry weight of each crucible was recorded. Then, the samples were combusted at 550 °C for three hours, plus one hour of ramp time. After the crucibles cooled, the combusted weight was recorded for each crucible. Finally, to burn off carbonates, samples were combusted at 950 °C for one hour, plus two hours of ramp time. Once cooled, this final combusted weight was recorded for each crucible. To find the dry bulk density

(DBD) of the samples, the dry mass (m_{dry}) was divided by the volume of each aliquot, 1.131 cm^3 (Eq. 1). To then find the percent loss on ignition at $550 \text{ }^\circ\text{C}$ (%LOI₅₅₀), Eq. 2 was utilized, which incorporates m_{dry} and the mass of the samples after the $550 \text{ }^\circ\text{C}$ burn (m_{550}) (Craft et al. 1991). Equation 3 was used to quantify the percent OC (%OC) in the matter that was lost on ignition; this equation was developed by Radabaugh et al. (2018) using soil from restored salt marshes in Tampa Bay.

$$\text{Equation 1: } DBD = \frac{m_{dry}}{1.131}$$

$$\text{Equation 2: } \%LOI550 = 100 \times \left(\frac{m_{dry} - m_{550}}{m_{dry}} \right)$$

$$\text{Equation 3: } \%OC = \%LOI550 \times 0.53587$$

To determine the total amount of carbon stored within the soil and vegetation at each site, the amount of carbon from all pools (soil and vegetation) was added together to give a final carbon (OC) stock. From here, the total OC stock was graphed against the site age to determine the rate of carbon sequestration.

Data Analysis

Statistical analyses were conducted using SAS Enterprise Guide 7.1 (SAS Institute Inc., Copyright © 2016, Cary, NC). Results were considered significant when statistical probabilities (p-values) were ≤ 0.05 . When a significant relationship was detected between two variables, graphs were fit with a trendline using Microsoft Excel (Microsoft Corporation, Copyright © 2016, Redmond, WA). The trendline chosen was based on whichever equation yielded the highest R^2 value. Tests utilized to test the significance of data include: Pearson product-moment correlation analyses, linear regressions, independent sample t-tests, paired t-tests, and one-way analyses of variance (ANOVAs) with post-hoc Tukey's tests.

Results

Remote Imagery

Based on available remote imagery, the extent of mangrove fringe was found to increase at seven of the ten sites, enabling calculation of the rate of inland mangrove encroachment per year (Table 1, Fig. 2). No mangroves were visible in satellite imagery of the three youngest sites (Perico Preserve, Rock Ponds, Perico Preserve 2). A positive trend was observed between site age and encroachment rate ($r = 0.69738$, $df = 8$, $p = 0.0250$; Fig. 3a), but this analysis included the three youngest sites, which did not have any mangrove trees. When the young sites were removed from analysis, there was no difference between the encroachment rate at middle-aged and old sites (2-sample $t = -0.4977$, $df = 5$, $p = 0.4977$; Fig. 3b). The average rate of encroachment across the seven sites with measurable mangrove fringe was $0.62 \pm 0.06 \text{ m y}^{-1}$.

Biotic Factors

Mangrove total ($paired t = 3.88$, $df = 9$, $p = 0.0037$) and basal ($paired t = 4.29$, $df = 9$, $p = 0.0020$) percent cover increased from 2016 to 2017. There was also an increase in herbaceous basal percent cover ($paired t = 2.81$, $df = 9$, $p = 0.0205$), but not in herbaceous total percent cover over the sampling period ($paired t = 1.84$, $df = 9$, $p = 0.0987$). No correlations were observed between site age and total percent cover of mangroves ($r = 0.59628$, $df = 8$, $p = 0.0688$; Fig. 4a) and herbaceous vegetation ($r = -0.50106$, $df = 8$, $p = 0.1401$; Fig. 4b). Similarly, no relationships were detected between site age and basal

percent cover of mangroves ($r = 0.19536$, $df = 8$, $p = 0.5886$; Fig. 4a) and herbaceous vegetation ($r = -0.36188$, $df = 8$, $p = 0.3042$; Fig. 4b).

Neither tree height (*paired t* = -1.01, $df = 9$, $p = 0.3394$) nor tree density (*paired t* = -1.54, $df = 9$, $p = 0.1575$) increased significantly over the sampling period. When compared to site age, though, tree height displayed a positive linear correlation ($r = 0.89565$, $df = 8$, $p = 0.0005$; Fig. 5a). No relationships were observed between site age and tree density ($r = 0.38080$, $df = 8$, $p = 0.2777$; Fig. 5b) and basal area ($r = 0.34662$, $df = 8$, $p = 0.3265$; Fig. 5c).

To calculate aboveground biomass, several novel allometric equations were generated relating stem height to dry weight (Table 2). Total aboveground vegetative biomass was then compared across the ten sites, but no significant difference was detected over the year-long sampling period (*paired t* = 0.46, $df = 9$, $p = 0.6571$). Traditional quadrat sampling revealed that there were no significant increases in the biomass of mangrove scrubs (*paired t* = 0.13, $df = 9$, $p = 0.8987$), trees (*paired t* = 0.23, $df = 9$, $p = 0.8217$), seedlings (*paired t* = 2.21, $df = 9$, $p = 0.0544$), or *S. alterniflora* (*paired t* = -0.68, $df = 9$, $p = 0.5129$) over the sampling period.

No differences were detected in the biomass of mangrove scrubs ($F = 4.67$, $df = 2$, 9 , $p = 0.0514$; Fig. 6a) or trees ($F = 3.14$, $df = 2$, 9 , $p = 0.1065$; Fig. 6b) at young, middle-aged, and old sites. Conversely, the biomass of mangrove seedlings ($F = 5.31$, $df = 2$, 9 , $p = 0.0395$; Fig. 6c) and *S. alterniflora* ($F = 5.15$, $df = 2$, 9 , $p = 0.0421$; Fig. 6d) was variable amongst the three age groups. *S. alterniflora* biomass was greatest at younger sites and negligible at older sites. Middle-aged sites had the greatest average mangrove seedling

biomass ($0.19 \pm 0.03 \text{ kg m}^{-2}$) and scrub biomass ($0.26 \pm 0.05 \text{ kg m}^{-2}$), while the biomass of seedlings and scrubs was lower in young and old sites.

Correlation analyses were performed to determine if relationships existed between site age and vegetative biomass, separated into four categories. No relationship was observed between site age and scrub biomass ($r = 0.08421$, $df = 8$, $p = 0.8171$; Fig. 7a), but a significant, positive correlation was detected between tree biomass and site age ($r = 0.67686$, $df = 8$, $p = 0.0316$; Fig. 7b), with older sites having the greatest tree biomass. A comparison of site age to the biomass of seedlings ($r = 0.20309$, $df = 8$, $p = 0.5736$; Fig. 7c) and *S. alterniflora* ($r = -0.61869$, $df = 8$, $p = 0.0565$; Fig. 7d) yielded no significant relationships.

Carbon Storage

Total OC storage was calculated across the ten sites (Table 3; Fig. 8) and a statistically significant difference between the total amount of OC stored in young, middle-aged, and old sites ($F = 5.68$, $df = 2, 9$, $p = 0.0343$; Fig. 9) was observed, with older sites storing the most OC ($125.0 \pm 13.9 \text{ Mg ha}^{-1}$). Linear regression analysis revealed a significant, positive relationship ($r = 0.94840$, $df = 8$, $p < 0.0001$; Fig. 10) between site age and average OC storage. The rate of sequestration, given by the slope of the least-squares regression, was $4.68 \text{ Mg C ha}^{-1} \text{ y}^{-1}$.

A statistically significant positive correlation between soil OC and vegetative OC was detected ($r = 0.72119$, $df = 8$, $p = 0.0186$; Fig. 11). To further analyze soil and vegetative OC, the Pearson product-moment correlation was calculated to determine whether relationships existed between OC storage and site age. No relationship was observed between soil OC and site age ($r = 0.56640$, $df = 8$, $p = 0.0878$; Fig. 12a), but a

significant, positive linear correlation existed between vegetative OC and site age ($r = 0.84362$, $df = 8$, $p = 0.0022$; Fig. 12b).

Soil DBD and OC% had a statistically significant, inverse relationship at young ($r = -0.20866$, $df = 504$, $p < 0.0001$; Fig. 13a), middle-aged ($r = -0.64839$, $df = 709$, $p < 0.0001$; Fig. 13b), and old sites ($r = -0.70071$, $df = 627$, $p < 0.0001$; Fig. 13c). Analysis of top 5-cm soil samples indicated that there was a significant difference in OC% ($F = 132.54$, $df = 19, 9$, $p < 0.0001$) and DBD ($F = 10.34$, $df = 19, 9$, $p = 0.0005$) across the ten restoration sites. Soil OC% ($F = 47.11$, $df = 5, 2$, $p = 0.0054$) and DBD ($F = 10.08$, $df = 5, 2$, $p = 0.0466$) were higher at plots closest to the water's edge. Finally, neither soil OC% (*paired* $t = -0.27$, $df = 59$, $p = 0.7858$) nor DBD (*paired* $t = 0.29$, $df = 59$, $p = 0.7745$) differed from 2016 to 2017.

Abiotic Factors

Grain size analysis was performed to find the total fraction of mud and sand within the top 5 cm of soil. The total abundance of sand did not change from 2016 to 2017 (*paired* $t = -1.44$, $df = 9$, $p = 0.1832$), but the mud size fraction increased over the sampling period (*paired* $t = -2.68$, $df = 9$, $p = 0.0253$). Correlation analyses determined that there was a negative relationship between site age and sand abundance ($r = -0.52524$, $df = 18$, $p = 0.0174$; Fig. 14a), but not the percentage of mud ($r = 0.50249$, $df = 8$, $p = 0.1388$; Fig. 14b). A full summary of abiotic factors, including depth to porewater, soil pH, open water salinity, porewater salinity, and open water DO% can be found in Appendix A.

Comparison to Natural Sites

OC storage (Mg ha^{-1}) was compared between the ten restored sites in this study, similar natural sites in Tampa Bay examined in Radabaugh et al. (2018), and natural sites

on Merritt Island along the eastern coast of Florida studied by Doughty et al. (2015). Natural salt marshes (Doughty et al. 2015; Radabaugh et al. 2018) and restored salt marshes (young sites in this study) exhibited no differences in aboveground OC (*2 sample t* = 2.94, *df* = 3, *p* = 0.0562; Table 4), belowground OC (*2 sample t* = 1.34, *df* = 5, *p* = 0.2382; Table 4), and total OC storage (*2 sample t* = 1.86, *df* = 5, *p* = 0.1218; Table 4). Similarly, no differences were detected between aboveground OC (*2 sample t* = -0.98, *df* = 3, *p* = 0.3977; Table 4), belowground OC (*2 sample t* = -0.27, *df* = 3, *p* = 0.8022; Table 4), and total OC storage (*2 sample t* = -0.57, *df* = 3, *p* = 0.6076; Table 4) at natural transitional sites on Merritt Island (Doughty et al. 2015) and restored transitional sites (middle-aged sites in this study). Finally, no differences were detected between natural mangrove sites (Doughty et al. 2015; Radabaugh et al. 2018) and restored mangrove sites (old sites in this study) with regards to aboveground OC (*2 sample t* = -1.75, *df* = 5, *p* = 0.1401; Table 4), belowground OC (*2 sample t* = 1.32, *df* = 3, *p* = 0.2785; Table 4), or total OC storage (*2 sample t* = -0.59, *df* = 5, *p* = 0.5812; Table 4).

Discussion

Analysis of Sampling Techniques

This study investigated characteristics of mangrove encroachment into restored salt marsh habitats using four different techniques: remote imagery analysis, PCQ sampling, traditional quadrat sampling via percent cover estimation, and biomass comparison via allometry. Satellite imagery was best suited to illustrate long-term vegetation changes at each site, as one year is not enough time to quantify significant mangrove expansion using ground-truthing techniques. Percent cover estimates were helpful in examining species composition of plots within the studied sites. While these estimates are subjective, they do provide the advantage of examining vegetation within and above the plots. Mangrove percent cover was found to be positively correlated with site age (Fig. 4a), and herbaceous percent cover was found to be negatively correlated with site age (Fig. 4b). These trends were expected, since mature salt marsh restoration sites are now mangrove-dominated, and contain little-to-no salt marsh vegetation, while younger sites still exhibit salt marsh characteristics (Osland et al. 2012).

Through biomass comparison, this study revealed that there was a difference in *S. alterniflora* biomass across young, middle-aged, and old sites (Fig. 6d). Salt marsh restoration sites are initially planted with *S. alterniflora*, which gradually declines in abundance after the first five to ten years as stems are shaded by a developing mangrove canopy (Osland et al. 2012), which explains why *S. alterniflora* was absent from the three oldest sites (EG Simmons, 27 years old; Mangrove Bay, 26 years old; and Harbor Palms,

23 years old). Hence, it is expected that middle-aged sites (Schultz Preserve (13), Cockroach Bay (12), Bishop Harbor (8), and Clam Bayou (6)) will soon exhibit further decline in *S. alterniflora* and other salt marsh vegetation and an increase in mangrove biomass (Osland et al. 2012).

Biomass comparison via allometry also revealed that middle-aged sites had the greatest average mangrove seedling biomass ($0.19 \pm 0.03 \text{ kg m}^{-2}$; Fig. 6c) and mangrove scrub biomass ($0.26 \pm 0.05 \text{ kg m}^{-2}$; Fig. 6a), as these sites are transitional ecotones. In this study, site age was positively correlated with tree height (Fig. 5a), with trees being the tallest at EG Simmons ($4.6 \pm 0.1 \text{ m}$), the oldest of the restoration sites (27 years old). EG Simmons displayed other characteristics typical of a mature restoration site, such as having a greater tree basal area than trees in younger sites ($12.4 \pm 0.7 \text{ m}^2 \text{ ha}^{-1}$ vs. $3.8 \pm 0.6 \text{ m}^2 \text{ ha}^{-1}$ at Cockroach Bay, 12 years old) and having no salt marsh vegetation. Doughty et al. (2015) observed that aboveground biomass was higher in sites with taller mangroves, but this was not always the case in this study. Mangrove biomass was typically higher in mature restoration sites (Figs. 6b and 7b), but it was higher than expected at Bishop Harbor (8 years old), a site which was not yet mangrove dominated. Trees at Bishop Harbor were not as tall as they were at older sites (Fig. 5a) but had basal areas ($17.3 \pm 1.3 \text{ m}^2 \text{ ha}^{-1}$) that were higher than average basal area at older restoration sites, ($10.4 \pm 1.2 \text{ m}^2 \text{ ha}^{-1}$; Fig. 5c), due to the presence of dense, young mangroves.

The PCQ methodology provided more accurate estimates of tree biomass (and thus, OC storage) than quadrat sampling in this study, as the small area surveyed by quadrats did not always contain tree trunks representative of the area. PCQ is a useful tool for modeling tree density and basal area, but it has limitations for short-term studies and in

mangrove forests. This study only measured trees over a year, which may not be enough time to observe noticeable differences in tree density, biomass, and basal area. Further, Dahdouh-Guebas and Koedam (2006) highlight issues with using PCQ methods to sample mangroves, as they tend to aggregate in dense clumps near the water's edge and exhibit size-concentric organization, which violates the assumption of random distribution. PCQ measurements also tend to vary widely depending on the individuals making the measurements, particularly in multi-stem trees or trees with unusual growth patterns (Dahdouh-Guebas and Koedam 2006). This sampling error, introduced during field surveys, makes it difficult to capture incremental changes over short timescales. Another issue with the PCQ method is that at least 50 sample points (up to 200 trees) are recommended to ensure a desired level of accuracy (Khan et al. 2016); however, only six sample points (a maximum of 24 trees) were measured at each site in this study. Further, Schultz Preserve exhibited the highest tree basal area ($39.6 \pm 15.1 \text{ m}^2 \text{ ha}^{-1}$), which was not an expected result, given its age of just 13 years at the time of this study. This discrepancy can be explained by the inclusion of large *Iva frutescens* trees when taking PCQ measurements. The inclusion of these trees does not appropriately represent the basal area of trees in the mangrove forest and is a limitation of this study and the PCQ methodology. The protocol does not indicate a maximum distance a tree can be from the center of the plot to be considered in a quarter of the quadrat (Cottam and Curtis 1956; Mitchell 2015).

Site Vulnerability to Mangrove Encroachment

The average rate of inland mangrove encroachment into restored salt marshes across the seven sites which had measurable mangrove fringe was found to be $0.62 \pm 0.06 \text{ m y}^{-1}$. Remote imagery revealed that the three youngest restoration sites (Perico Preserve,

Rock Ponds, and Perico Preserve 2, all 4 years old or younger) did not have any measurable mangrove fringe; however, within four years of site creation, the next youngest site (Clam Bayou, 6 years old), had 6.67 m of mangrove fringe (Table 1 and Fig. 2). Based on remote imagery analysis, this site had the fastest rate of mangrove encroachment (0.85 m y^{-1} ; Table 1). Middle-aged (6- to 13-year-old) restoration sites did not experience the fastest rate of mangrove encroachment; rather, there was no difference in the rate of mangrove expansion at restoration sites of different ages. This allows for acceptance of Null Hypothesis 1 and rejection of Hypothesis 1, which hypothesized that middle-aged sites would experience the fastest rate of mangrove encroachment, suggesting that rates of landward mangrove expansion within 27 years of site creation follow a linear trajectory.

One possible reason for the elevated rate of mangrove encroachment at Clam Bayou is propagule availability. In another Florida study, Stevens et al. (2006) concluded that mangrove seedling recruitment is largely dependent on a local source of propagules. The site with the highest rate of seedling recruitment ($76 \text{ seedlings m}^{-2} \text{ y}^{-1}$) received propagules from nearby mangroves (5 to 15 m away), which settled in adjacent salt marsh vegetation (Stevens et al. 2006). Analysis of the satellite imagery of Clam Bayou showed that it has direct hydrologic connection to nearby natural mangroves (100 m away; Fig. 2), which facilitates propagule dispersal into the site's restored salt marsh. Further, Kelleway et al. (2016) suspect that differences in salinity, nutrient limitation, and sedimentation may determine biomass response. For example, sites with lower salinities tend to exhibit increased growth of mangrove seedlings, and sedimentation prior to encroachment may enhance mangrove recruitment success (Kelleway et al. 2016). Conversely, Raabe et al. (2012) observed that salt marsh persisted in areas near freshwater sources. When not

limited by temperature, SLR and saline water intrusion have been demonstrated to be primary drivers in mangrove expansion (Comeaux et al. 2012; Raabe et al. 2012). Albeit, mangrove seedling density was not significantly correlated with porewater salinity, open water salinity, or pH in this study.

Further analysis of remote imagery showed that Schultz Preserve (13 years old) transitions from mangrove fringe to high marsh, characterized by *Spartina patens* (smooth cordgrass) and *Borrchia frutescens* (sea oxeye), but then quickly transitioned to upland vegetation. While this study did not collect elevation data, the steep slope at the transition to upland habitat may prevent further mangrove expansion at the present sea level, as higher elevations are not suitable for mangrove settlement (Fig. 2) (Stevens et al. 2006). Hence, Schultz Preserve may be less vulnerable to mangrove encroachment than Cockroach Bay, which is just one year younger. Both sites had high mangrove seedling density ($8.6 \pm 0.2 \text{ m}^{-2}$ at Cockroach Bay vs. $9.2 \pm 1.5 \text{ m}^{-2}$ at Schultz Preserve), but because it does not contain a steep slope transitioning to upland elevation, Cockroach Bay mangroves will likely migrate inland as sea levels rise. To support this, Cockroach Bay exhibited a higher encroachment rate (0.63 m y^{-1} ; Table 1) and mangrove tree biomass ($6.6 \pm 1.0 \text{ kg m}^{-2}$) than Schultz Preserve (0.49 m y^{-1} ; $3.7 \pm 0.2 \text{ kg m}^{-2}$; Table 1).

Harbor Palms had a lower mangrove density ($0.15 \pm 0.01 \text{ trees m}^{-2}$) and basal area ($5.8 \pm 0.4 \text{ m}^2 \text{ ha}^{-1}$) than expected, despite being an older site (23 years old). Harbor Palms was the longest transect (68 m) examined and included a broad salt barren (Fig. 2). Mangroves were notably stunted or absent in the salt barren, contributing to the low density and basal area of mangrove trees at this site. Porewater salinity in the salt barren was 59.2 ± 2.1 , while porewater salinity closest to the water's edge was considerably lower, $11.8 \pm$

3.6. Additionally, the nearest source of tidal water to this site was a small tidal tributary rather than a large body of open water. Thus, this relative hydrologic isolation may have slowed the delivery and initial recruitment of mangrove propagules to the site. Additionally, Kelleway et al. (2016) found that basin sites without direct access to an open body of water were often nutrient-poor, so mangrove growth was stunted. Thus, Harbor Palms was relatively resistant to mangrove encroachment.

Other sites that contained salt barrens included Bishop Harbor, Rock Ponds, Perico Preserve, and Perico Preserve 2. At the current sea level, the presence of a salt barren may prevent further mangrove expansion from occurring. However, as the sea level rises, and inundation becomes more frequent, salinity within the salt barren will decrease, which may facilitate mangrove expansion (Comeaux et al. 2012; Raabe et al. 2012). At the time of data collection, Rock Ponds, Perico Preserve, and Perico Preserve 2 were young sites (≤ 4 years old) and were dominated by herbaceous vegetation and have had limited time for seedling establishment. These sites are relatively isolated from a larger body of water, and therefore have low hydrologic connectivity to nearby mangroves (Fig. 2). Propagule dispersal is thus limited, which may cause these sites to be more resistant to mangrove encroachment now, as well as their current young age. However, as these sites mature, they are expected to slowly transition into mangrove forests.

Based on remote imagery analysis supported by PCQ measurements and allometry, the sites that were least vulnerable to mangrove encroachment at the time of this study were Harbor Palms, Schultz Preserve, Rock Ponds, Perico Preserve, and Perico Preserve 2. These sites exhibited several characteristics which allow them to be more resistant to mangrove encroachment, including: a lack of a hydrologic connection to nearby

mangroves, salt barren presence, existence of high marsh, and a steep slope at the transition between high marsh and upland vegetation. *S. alterniflora* is the most common species initially planted at coastal wetland restoration sites (Osland et al. 2012), but it also facilitates mangrove expansion by trapping propagules at low elevations and providing a warmer layer that protects seedlings from cold temperatures (Guo et al. 2013; Smee et al. 2017). Thus, if restoration practitioners are interested in creating a salt marsh that is resistant to mangrove expansion, coastal managers should incorporate a salt barren and/or high marsh vegetation, which usually exist at elevations not suitable for mangroves (Guo et al. 2013). This solution is only temporary, but it provides the benefit of a low marsh now while allowing mangroves to become dominant in the face of SLR.

Impacts of Mangrove Encroachment

Salt marshes and mangroves differ in their above- and belowground structure, ability to trap allochthonous materials and deposit OM, and rates of carbon cycling (Kelleway et al. 2017). This alters coastal structure, which may provide new challenges and opportunities to coastal managers. For example, mangrove encroachment is suspected to enhance coastal resilience to storms. Mangroves act as a wind break (Shaffer et al. 2009), increase wave attenuation due to their stem stiffness and larger stature (Bouma et al. 2005; Kelleway et al. 2017), and are less likely to become submerged during storm surges than their marsh counterparts (Feller et al. 2015). Mangroves may also be better suited to adapt to accelerating SLR, as they have been shown to foster vertical accretion faster than salt marshes (Kelleway et al. 2017).

Mangroves provide many of the same ecosystems services as salt marshes, but this enhanced encroachment may pose challenges to salt-marsh-dependent organisms. Salt

marshes serve as critical nursery habitats for *Callinectes sapidus* (blue crab), *Centropomus undecimalis* (snook), *Nerodia clarkii* subsp. (salt marsh snakes), and *Elops saurus* (ladyfish) (Robison et al. 2010). A reduction of salt marsh, then, will create a habitat deficiency over the life histories of these species. Salt-marsh-dependent birds, such as *Ammospiza maritima* (seaside sparrows) and *Cistothorus palustris* (long-billed marsh wrens), may leave the area as salt marshes are replaced by mangroves and roosting habitat is lost (Stevens et al. 2006; Kelleway et al. 2017). It has also been observed that upper intertidal salt marshes have a higher concentration of invertebrate larvae than mangroves, which provides ample feeding opportunities for zooplanktivorous fish (Mazumder et al. 2009). With continued mangrove encroachment, this abundant food source will be lost for zooplanktivorous fish. Additionally, Smee et al. (2017) observed that *Palaemonetes* sp. (grass shrimp), *Penaeus aztecus* (brown shrimp), and *C. sapidus* were more abundant in salt marshes than in mangrove forests in Rockport, Texas, so mangrove expansion may inhibit the survival of these organisms as well. The loss of suitable habitat changes the foraging environment for predators and prey, which alters food web interactions and may have long-term consequences on the ecosystem (Smee et al. 2017).

Mangrove encroachment will have many different impacts on coastal wetlands across Florida. While it is difficult to predict exactly how these ecosystems will respond to future warming and SLR, mangrove encroachment is expected to continue in the future, further altering species composition, abundance, and distribution (Robison et al. 2015). Thus, it may not be feasible, nor realistic to “restore the balance” of Tampa Bay coastal habitats as currently planned (Duarte et al. 2009). Rather, Robison et al. (2015) suggest that comprehensive, long-range planning should be implemented to ensure the future

integrity of Tampa Bay's coastal wetland communities. This involves identifying, prioritizing, and conserving low-lying, undeveloped coastal uplands as buffer zones, which allows for the landward migration of coastal wetland habitats (Robison et al. 2015).

Carbon Storage

As sites mature and become mangrove dominated, aboveground and belowground vegetative biomass increases, which increases the total OC stock (Doughty et al. 2015; Kelleway et al. 2016). Additionally, soil OC increases with mangrove fine root development, while DBD decreases as root biomass exceeds sediment volume (Osland et al. 2012; Kelleway et al. 2016). Comparatively, Breithaupt et al. (2017) found that DBD is largely driven by the rate of soil inorganic matter accumulation, while the rate of soil organic matter predicted the rate of accretion in areas of high allochthonous carbon input and sedimentation. In this study, soils from younger restoration sites exhibited higher DBD and lower OC storage ($33.5 \pm 7.6 \text{ Mg ha}^{-1}$) than older sites ($67.3 \pm 0.8 \text{ Mg ha}^{-1}$). Vegetative OC was also greater in older sites ($71.5 \pm 14.4 \text{ Mg ha}^{-1}$), as marsh vegetation is replaced by woody vegetation and aboveground biomass increases. This allows for the rejection of Null Hypothesis 2, and acceptance of Hypothesis 2, which stated that old restoration sites would have the highest soil and vegetative OC stocks.

Doughty et al. (2015) examined mangrove encroachment along Florida's east coast and observed similar trends in OC storage and soil characteristics. Similar to this study, Doughty et al. (2015) found that total OC stocks were considerably higher in mangrove-dominated sites than in salt marshes or transitional ecosystems (Table 4; Fig. 9). Doughty et al. (2015) also noted that taller mangroves (> 2 m) stored more OC than scrub (dwarf) mangroves. This study supports this claim, as vegetative OC storage was higher in sites

with taller trees, such as EG Simmons and Mangrove Bay (Figs. 5a and 12b), except for Bishop Harbor, a site which had high vegetative OC due to dense, short mangroves. Additionally, sites with noticeably shorter mangroves (< 2.5 m), such as Harbor Palms, had a low vegetative OC (< 50 Mg ha⁻¹).

Bishop Harbor exhibited higher soil OC than would be expected by site age (Figs. 8 and 12b). This is likely because the substrate used to create the restoration site contained a large amount of clay, whereas most other sites in this study were created using sand. Bishop Harbor had a larger percentage of mud (2.5 ± 0.1 %; Fig. 14b) than the average percentage of mud across the other sites (1.6 ± 0.3 %). During LOI analysis, soils that contain clay minerals have been found to lose water at higher temperatures after the initial drying stage at 105 °C, resulting in a loss of both water and OM at the 550 °C burn (Barillé-Boyer et al. 2003; Howard et al. 2014). This causes an overestimation of OM, and thus, OC. Soil data for Bishop Harbor are therefore inaccurate and were removed from Fig. 10 to improve estimates of the rate of carbon sequestration. Soil data were included in Fig. 8 for visual comparison purposes, but more research needs to be done to create an appropriate clay conversion factor specific to Tampa Bay ecosystems to correct for the overestimation of OC.

One of the limitations of this study is that it did not specifically examine belowground vegetative biomass or OC other than through LOI analysis. Belowground root biomass is prominent in mangroves and may contribute up to 60 % of the total biomass (Khan et al. 2009; Adame et al. 2017). It is therefore believed that mangroves invest more fixed carbon to their root system compared to other woody vegetation to maximize water uptake, retain nutrients, transport oxygen, and increase stability in hydric soils (Adame et

al. 2017). Field measurements of root biomass are labor-intensive and not always feasible, so allometric equations can be used to estimate vegetative biomass belowground. However, these estimations are clouded with uncertainty, since they rely on aboveground measurements, and provide higher estimations of root biomass (on average 40 % higher) than roots measured in the field (Adame et al. 2017). While roots are integral to coastal wetland ecosystems, it has been found that they only account for 1 to 16 % of the total carbon stock (Adame et al. 2015; Adame et al. 2017). Moreover, belowground carbon of salt marshes and mangroves is estimated through LOI analysis, which encompasses soil and fine roots (Radabaugh et al. 2018). For these reasons, belowground biomass was not examined in this study, but may provide more accurate comparisons to published OC stock values (Howard et al. 2014).

Coastal wetland restoration projects have the potential to become significant sources of carbon sequestration in Florida (Stevens et al. 2011). Afforestation/reforestation was one of the state's main policies under the Governor's Energy and Climate Change Action Plan, implemented by former Governor Charlie Crist with an aim to increase the area of forested lands by 20,200 ha and implement reforestation activity on all harvested areas by 2025 (GATECC 2008; Stevens et al. 2011). If these goals are met, atmospheric GHG levels could be reduced by 134 million metric tons of CO₂ or CO₂ equivalent (CO₂e) (GATECC 2008; Stevens et al. 2011). However, the current plan does not distinguish between upland forests and mangrove forests, so Stevens et al. (2011) suggest that a broader afforestation offset program, which covers all land and vegetation types, be implemented. Stevens et al. (2011), Gardner and Fox (2013), and Sutton-Grier and Moore (2016) all recommend that GHG emission offset programs, which provide financial

incentives to landowners, would promote the interest in wetland restoration programs, as wetlands store more carbon than other ecosystems.

Carbon Sequestration

This study complements Radabaugh et al. (2018) carbon stock study by examining a chronosequence of restoration sites in the Tampa Bay Estuary to gain a better understanding of how mangrove encroachment affects soil and vegetative OC storage at ecological restoration sites. Site age was compared to total OC storage and the average rate of carbon sequestration across the 26-year chronosequence was found to be $4.68 \text{ Mg C ha}^{-1} \text{ y}^{-1}$ (Fig. 10). While some studies have examined rates of belowground carbon sequestration in established wetlands using radiometric dating (Chmura et al. 2003; Alongi 2014; Breithaupt et al. 2014; Marchio et al. 2016), no studies were found that calculated the rate of sequestration in restored or created wetlands.

Using radiometric dating, Marchio et al. (2016) found that the average rate of belowground OC sequestration ranged from $0.47 \pm 0.04 \text{ Mg C ha}^{-1} \text{ y}^{-1}$ in disturbed watersheds to $1.62 \pm 0.05 \text{ Mg C ha}^{-1} \text{ y}^{-1}$ in undisturbed watersheds in long-standing mangrove forests in Naples, FL. However, Marchio et al. (2016) did not include aboveground OC storage when calculating the rate of carbon sequestration; rather, soil cores and ^{210}Pb dating were used to model rates of carbon sequestration over a 50-year time period. In another south Florida study, Breithaupt et al. (2014) found the belowground rate of carbon sequestration in natural mangroves in the Everglades to be $1.23 \pm 0.19 \text{ Mg C ha}^{-1} \text{ y}^{-1}$ over a 100-year period using a similar dating method. However, the rates of carbon sequestration presented by Marchio et al. (2016) and Breithaupt et al. (2014) are slightly lower than the global belowground average of $1.74 \text{ Mg C ha}^{-1} \text{ y}^{-1}$ suggested by Alongi

(2014). In another study, Chmura et al. (2003) estimated the global soil carbon sequestration rate in salt marshes and mangroves at $2.1 \text{ Mg CO}_2\text{e ha}^{-1} \text{ y}^{-1}$. This study found the belowground OC sequestration rate to be $1.57 \text{ Mg C ha}^{-1} \text{ y}^{-1}$ over the 26-year chronosequence, similar to the rates reported in natural, undisturbed mangroves and marshes. While radiometric dating was not utilized, an advantage of this study is that the true age of the sites is known, which allowed for precise calculation of both belowground and aboveground rates of OC sequestration.

Comparison to Natural Sites

While restoration sites do not perfectly mimic natural sites, they do provide a variety of ecosystem services. In this study, sites began to exhibit growth of predominantly woody vegetation 6 to 10 years after creation and contained minimal salt marsh vegetation after six years of creation (Fig. 8). Natural mangrove forests require 20 to 30 years to reach full maturity, but restored sites may require more time (Shafer and Roberts 2008; Osland et al. 2012). Edwards and Proffitt (2003) noticed that it only takes around five years for the plant species composition of restored salt marshes to be similar to that of natural sites, as herbaceous vegetation matures faster than trees, suggesting that Perico Preserve (4 years old), Rock Ponds (1), and Perico Preserve 2 (1) are still maturing marshes. Osland et al. (2012) observed that forest density and tree DBH were still increasing in restoration sites over 20 years old, so it is possible that EG Simmons (27 years old), Mangrove Bay (26), and Harbor Palms (23) have not yet reached forest maturity. In fact, Osland et al. (2012) projected that it can take as long as 55 years for mangrove trees to reach a comparable density and 25 years to reach a similar DBH to that of natural sites.

Osland et al. (2012) also noticed significant differences in the soil composition of natural and created sites. The soils of created or restored sites in their study had higher pH in the top 10 cm (6.8 ± 0.1 , restored vs. 6.2 ± 0.1 , natural), larger sand fraction, higher DBD, and lower total carbon and total nitrogen than natural reference sites, all characteristic of the sandy substrate used to create the wetlands. Osland et al. (2012) attributed these differences to vegetation variability; as the vegetation transitions from predominantly salt marsh to mangrove, peat begins to accumulate in the upper soil layers, which is rich in carbon and nitrogen. Furthermore, this study found the average soil pH across all restoration sites to be 6.36 ± 0.05 (App. A), which is not nearly as high as the restored pH value presented in Osland et al. (2012). This study also found that no relationship existed between site age and pH in the top 5 cm of soil (App. A), possibly because the sites are still relatively young and soil characteristics are still maturing. Although, after about 20 years, Osland et al. (2012) observed that soil characteristics began to resemble peat found in natural sites, with lower dry bulk densities, lower pH values, and greater amounts of OC and nitrogen. Edwards and Proffitt (2003) also observed higher amounts of OC in the oldest restored marshes, while younger sites exhibited greater DBD. This study observed similar relationships, as a negative correlation between site age and sand percentage was observed (Fig. 14a). Differences were also noted in soil OC% and DBD across young, middle-aged, and old restoration sites, with older sites having the greatest average OC% (5.0 ± 0.3 %, compared to 1.1 ± 0.0 % in young sites) and lowest DBD (0.86 ± 0.02 g cm⁻³, compared to 1.1 ± 0.0 g cm⁻³ in young sites). For all soil cores collected, a negative correlation was observed between OC% and DBD (Figs. 13a, b, and c).

Furthermore, natural salt marshes along Florida's Gulf Coast are dominated by *J. roemerianus* a mesohaline tidal marsh plant (Stout 1984; Raabe et al. 2012). Unlike *S. alterniflora*, which is the vegetation often initially planted at restoration sites, *J. roemerianus* is typically found at higher elevations and lower interstitial salinities (Stout 1984; Pennings et al. 2005; Raabe et al. 2012). Unlike *S. alterniflora*, *J. roemerianus* is a slow-growing plant and has extensive belowground root reserves, causing it to respond slower to abiotic fluctuations (Pennings et al. 2005). *J. roemerianus* was only present at one site in this study, Mangrove Bay. While its abundance was low, mangrove seedlings were absent in the surrounding area. Therefore, the inclusion of high marsh species in coastal wetland restoration plans may increase marsh resilience.

Total OC stocks calculated in this study were compared to OC stocks of natural sites examined by Radabaugh et al. (2018) and Doughty et al. (2015). No statistically significant differences were detected in soil, vegetative, or total OC (Table 4). However, the minimum OC content in natural Tampa Bay salt marshes was 45.2 Mg C ha⁻¹ (Radabaugh et al. 2018), which is still higher than the maximum 42.2 Mg C ha⁻¹ observed in restored sites. This lack of statistical significance is likely attributed to the small sample sizes in the three studies. Radabaugh et al. (2018) estimated that a total of 996,000 Mg C ha⁻¹ is stored in Tampa Bay's wetland ecosystems and concluded that mangrove expansion will increase carbon sequestration over time. Because salt marshes and barrens have lower average carbon stocks than mangroves in Tampa Bay, mangrove encroachment will increase carbon stocks (SWFWMD 2012; Radabaugh et al. 2018). The present study supports this claim; OC storage increased with site age as mangroves became the dominant habitat (Fig. 10). This relationship yielded a carbon sequestration rate across soil and

vegetative OC pools of $4.68 \text{ Mg C ha}^{-1} \text{ y}^{-1}$, and is the first known study to consider vegetative (aboveground) OC storage when calculating the sequestration rate. It is also the first known study to examine OC storage in restored wetlands.

Conclusion

This study investigated characteristics of mangrove encroachment into ten restored salt marsh habitats adjacent to the Tampa Bay Estuary using four different techniques: remote imagery analysis, PCQ sampling, traditional quadrat sampling via percent cover estimation, and biomass comparison via allometry. The rate of mangrove encroachment was determined through remote imagery, and it was hypothesized that middle-aged (6- to 13-year-old) restoration sites would experience the fastest rate of mangrove encroachment. The average mangrove encroachment rate was found to be $0.62 \pm 0.06 \text{ m y}^{-1}$, but no difference was found between the encroachment rate at old (14- to 27-year-old) and middle-aged sites, suggesting that rates of landward mangrove expansion within 27 years of site creation follow a linear trajectory.

After calculating the rate of inland mangrove encroachment at the ten salt marsh restoration sites, characteristics of each site were examined to assess their vulnerability to future mangrove expansion. Sites that were deemed most resistant to mangrove encroachment included one or more of the following: high marsh vegetation, a salt barren, a steep slope at the transition between high marsh and upland vegetation, or lacked a hydrologic connection to nearby mangroves. It is therefore recommended that coastal managers include high marsh vegetation and/or a salt barren in coastal wetland restoration projects, as this provides a location for low marsh vegetation and mangroves to move upslope in the face of SLR.

The second objective of this study was to calculate a total carbon stock for each site. It was hypothesized that old restoration sites would store the most OC. Carbon stocks were calculated with the use of allometric calculations, PCQ analysis, and soil core analyses. Mangrove-dominated restoration sites were found to have higher total carbon stocks ($138.7 \pm 13.8 \text{ Mg C ha}^{-1}$) than middle-aged transitional sites ($85.6 \pm 25.5 \text{ Mg C ha}^{-1}$) or young salt marshes ($34.5 \pm 7.7 \text{ Mg C ha}^{-1}$), demonstrating that carbon storage increases with site age. These carbon stocks were similar to those of natural coastal wetlands in the Tampa Bay Estuary (Radabaugh et al. 2018) and along Florida's east coast (Doughty et al. 2015).

Using the calculated OC storage, the carbon sequestration rate across the 26-year chronosequence was found to be $4.68 \text{ Mg C ha}^{-1} \text{ y}^{-1}$. This value is higher than belowground rates of carbon sequestration calculated values in other Florida studies (Breithaupt et al. 2014; Marchio et al. 2016), as it includes both vegetative and soil OC storage, making it the first known study to do so. Given global and regional soil carbon sequestration rates, studies have shown that the conservation and restoration/creation of mangroves is economically viable (Siikamäki et al. 2012; Mack et al. 2014; Vázquez-González et al. 2017). This may incentivize coastal managers to pursue wetland restoration projects, knowing that they can partially reduce atmospheric CO_2 while simultaneously generating revenue. The carbon sequestration rate calculated in this study provides a unique rate for the Tampa Bay area, and may stimulate further interest in initiating a carbon market.

TABLES

Table 1. Mangrove encroachment rates (m y^{-1}) into salt marsh restoration sites. Encroachment rates were determined using Google Earth imagery.

Site and Abbreviation	Year planted	Past photo date	Mangrove thickness (m)	Present photo date	Mangrove thickness (m)	Encroachment rate (m y^{-1})	Transect Length (m)
EG Simmons (EG)	1990	2002-04-30	22.2	2017-09-14	34.0	0.77	31.0
Mangrove Bay (MB)	1991	2002-04-30	9.85	2017-09-14	19.8	0.65	27.4
Harbor Palms (HP)	1994	2002-04-30	16.5	2017-09-14	25.7	0.60	68.0
Schultz Preserve (SP)	2004	2007-12-18	7.63	2017-09-14	12.4	0.49	16.0
Cockroach Bay (CR)	2005	2012-04-24	6.33	2017-09-14	9.75	0.63	15.4
Bishop Harbor (BH)	2009	2010-12-01	4.41	2017-09-14	6.85	0.36	20.5
Clam Bayou (CB)	2011	2013-03-14	3.40	2017-01-11	6.67	0.85	19.5
Perico Preserve (PP)	2013	2016-02-04	0.00	2017-01-07	0.00	0.00	15.0
Rock Ponds (RP)	2016	2016-02-12	0.00	2017-09-14	0.00	0.00	24.0
Perico Preserve 2 (PP2)	2016	2016-02-04	0.00	2017-01-07	0.00	0.00	8.00

Table 2. Novel allometric equations generated in this study. These equations were used to calculate aboveground biomass (b , g) from stem height (ht , cm).

Species	Common Name	Allometric Equation	R ² value	Number of specimens
<i>Cyperus esculentus</i>	Yellow nutsedge	$\ln(b) = 2.0813 \ln(ht) - 6.4251$	0.8647	25
<i>Cyperus rotundus</i>	Purple nutsedge	$\ln(b) = 0.8651 \ln(ht) - 4.4539$	0.5260	61
<i>Dichanthelium</i> sp.	Rosette grass	$\ln(b) = 1.8048 \ln(ht) - 6.1295$	0.7053	43
<i>Distichlis spicata</i>	Saltgrass	$\ln(b) = 1.2539 \ln(ht) - 5.6389$	0.7946	52
<i>Panicum</i> sp.	Switchgrass	$\ln(b) = 1.1238 \ln(ht) - 5.1012$	0.6423	53
<i>A. germinans</i> pneumatophore	Black mangrove pneumatophore	$b = 0.3008e^{0.0768(ht)}$	0.8585	53
<i>S. terebinthifolius</i> seedling	Brazilian pepper seedling	$b = 0.0007(ht) - 8 \times 10^{-5}$	0.3675	63
<i>Scoparia dulcis</i>	Licorice weed	$\ln(b) = 2.0325 \ln(ht) - 7.1049$	0.8215	37
<i>Seutera angustifolia</i>	Gulf coast swallowwort	$b = 0.0041(ht) - 0.0773$	0.7563	40
<i>Spartina bakeri</i>	Sand cordgrass	$\ln(b) = 1.928 \ln(ht) - 7.8901$	0.8909	44
<i>Suaeda linearis</i>	Annual seepweed	$\ln(b) = 2.3682 \ln(ht) - 7.8355$	0.8126	27
<i>Triglochin striata</i>	Arrowgrass	$\ln(b) = 1.4639 \ln(ht) - 6.5292$	0.6781	44
<i>Vigna luteola</i>	Hairy pod cowpea	$\ln(b) = 1.6325 \ln(ht) - 6.9224$	0.8894	17

Table 3. Vegetative and soil organic carbon (OC) (Mg ha⁻¹) storage at each restoration site. The error shown is \pm SE.

Site	Scrub OC	Seedling OC	Mangrove tree OC	Non-mangrove tree OC	Salt marsh OC	Standing dead wood OC	Pneumatophore OC	Total vegetative OC	Soil OC	Total OC
EG Simmons	0.53 \pm 0.00	1.82 \pm 0.04	94.6 \pm 1.0	0.6 \pm 0.0	0.00 \pm 0.00	7.83 \pm 0.16	0.45 \pm 0.02	105.8 \pm 11.7	66.2 \pm 0.1	171.9 \pm 12.3
Mangrove Bay	0.01 \pm 0.00	0.59 \pm 0.01	29.4 \pm 1.2	30.4 \pm 1.2	0.05 \pm 0.01	0.36 \pm 0.04	0.76 \pm 0.04	61.6 \pm 4.9	66.5 \pm 0.1	128.1 \pm 8.1
Harbor Palms	0.23 \pm 0.01	1.46 \pm 0.01	38.3 \pm 0.7	6.6 \pm 0.2	0.27 \pm 0.00	0.00 \pm 0.00	0.19 \pm 0.00	47.0 \pm 4.7	69.1 \pm 0.1	116.2 \pm 8.5
Schultz Preserve	1.80 \pm 0.00	3.52 \pm 0.05	15.2 \pm 0.2	5.5 \pm 0.0	0.05 \pm 0.00	0.08 \pm 0.00	0.17 \pm 0.01	26.4 \pm 1.9	57.5 \pm 0.1	83.9 \pm 6.5
Cockroach Bay	0.80 \pm 0.00	3.51 \pm 0.04	29.3 \pm 0.4	0.0 \pm 0.0	0.30 \pm 0.01	0.00 \pm 0.00	0.57 \pm 0.04	34.5 \pm 3.6	43.1 \pm 0.1	77.5 \pm 5.6
Bishop Harbor	1.22 \pm 0.01	0.71 \pm 0.02	59.0 \pm 1.4	0.0 \pm 0.0	0.17 \pm 0.00	0.00 \pm 0.00	0.12 \pm 0.01	61.2 \pm 7.3	91.3 \pm 0.1	152.4 \pm 11.8
Clam Bayou	0.43 \pm 0.00	1.21 \pm 0.03	8.1 \pm 0.3	0.3 \pm 0.0	0.23 \pm 0.00	0.00 \pm 0.00	0.53 \pm 0.04	10.8 \pm 1.0	17.7 \pm 0.0	28.5 \pm 2.1
Perico Preserve	0.00 \pm 0.00	0.01 \pm 0.00	0.0 \pm 0.0	0.0 \pm 0.0	0.26 \pm 0.01	0.00 \pm 0.00	0.00 \pm 0.00	0.3 \pm 0.0	32.4 \pm 0.1	32.6 \pm 3.8
Rock Ponds	0.04 \pm 0.00	0.72 \pm 0.01	0.0 \pm 0.0	0.0 \pm 0.0	0.75 \pm 0.04	0.00 \pm 0.00	0.00 \pm 0.00	1.5 \pm 0.1	50.1 \pm 0.0	51.6 \pm 5.8
Perico Preserve 2	0.00 \pm 0.00	0.05 \pm 0.01	0.0 \pm 0.0	0.0 \pm 0.0	1.02 \pm 0.02	0.00 \pm 0.00	0.00 \pm 0.00	1.1 \pm 0.1	18.0 \pm 0.1	19.1 \pm 2.1

Table 4. Comparison of organic carbon (OC) stocks (Mg ha^{-1}) in restored and natural salt marshes, transitional habitats, and mangroves. Restored sites ≤ 5 years old (young sites) were considered salt marsh habitat. Restored sites 6-to-13 years old (middle-aged sites) were considered transitional habitat. Restored sites ≥ 14 years old (old sites) were considered mangrove habitat in this study.

Site	Reference	Average OC (Mg ha^{-1})		
		Aboveground	Belowground	Total
Salt marshes				
Tampa Bay, FL natural salt marsh	Radabaugh et al. 2018	6.7 ± 2.3	93.8 ± 33.4	100.5 ± 35.7
Merritt Island, FL natural salt marsh	Doughty et al. 2015	8.0 ± 1.0	52.0 ± 6.0	60.0 ± 4.0
Tampa Bay, FL restored salt marsh	This study	1.0 ± 0.3	33.5 ± 7.9	34.5 ± 7.7
Transitional habitats				
Merritt Island, FL natural transitional habitat	Doughty et al. 2015	10.0 ± 1.0	43.0 ± 5.0	53.0 ± 5.0
Tampa Bay, FL restored transitional habitat	This study	33.2 ± 10.5	52.4 ± 15.3	85.6 ± 25.5
Mangroves				
Tampa Bay, FL natural mangrove	Radabaugh et al. 2018	40.1 ± 3.2	88.0 ± 12.1	128.1 ± 14.5
Merritt Island, FL natural mangrove	Doughty et al. 2015	55.0 ± 11.0	67.0 ± 9.0	122.0 ± 16.0
Tampa Bay, FL restored mangrove	This study	71.5 ± 14.4	67.3 ± 0.8	138.8 ± 13.8

FIGURES

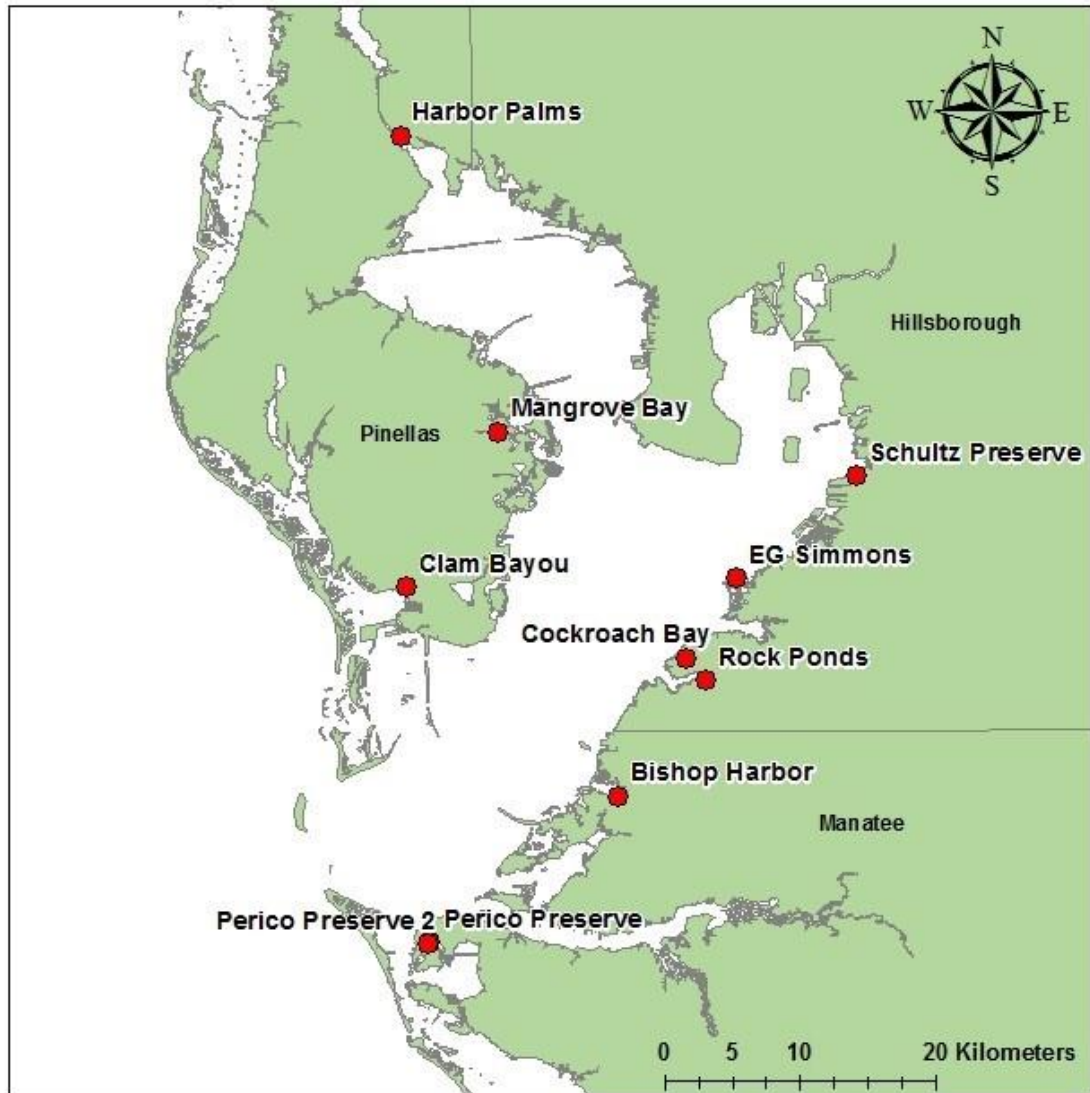














Figure 1. Locations of the ten restored coastal wetlands in Tampa Bay that were examined in this study (Source: Environmental Systems Research Institute (ESRI), Copyright © 2017, ArcGIS Release 10.5.1, Redlands, CA).

Site and Date	Past Photo	Present Photo
<p>EG Simmons 2002/2017</p>		
<p>Mangrove Bay 2002/2017</p>		
<p>Harbor Palms 2002/2017</p>		

<p>Schultz Preserve 2007/2017</p>		
<p>Cockroach Bay 2012/2017</p>		
<p>Bishop Harbor 2010/2017</p>		






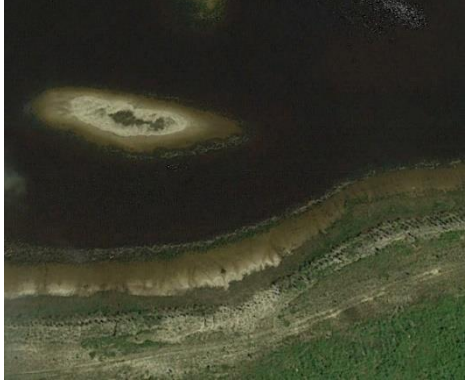
<p>Clam Bayou 2013/2017</p>		
<p>Perico Preserve 2016/2017</p>		
<p>Rock Ponds 2016/2017</p>		



Figure 2. Aerial imagery of the ten restoration sites in the past and near-present. The thin white lines signify the mangrove fringe width that was measured along the vegetation transect, if present (Source: Google Earth v. 7.1.8.3036. Google Inc., Copyright © 2017).

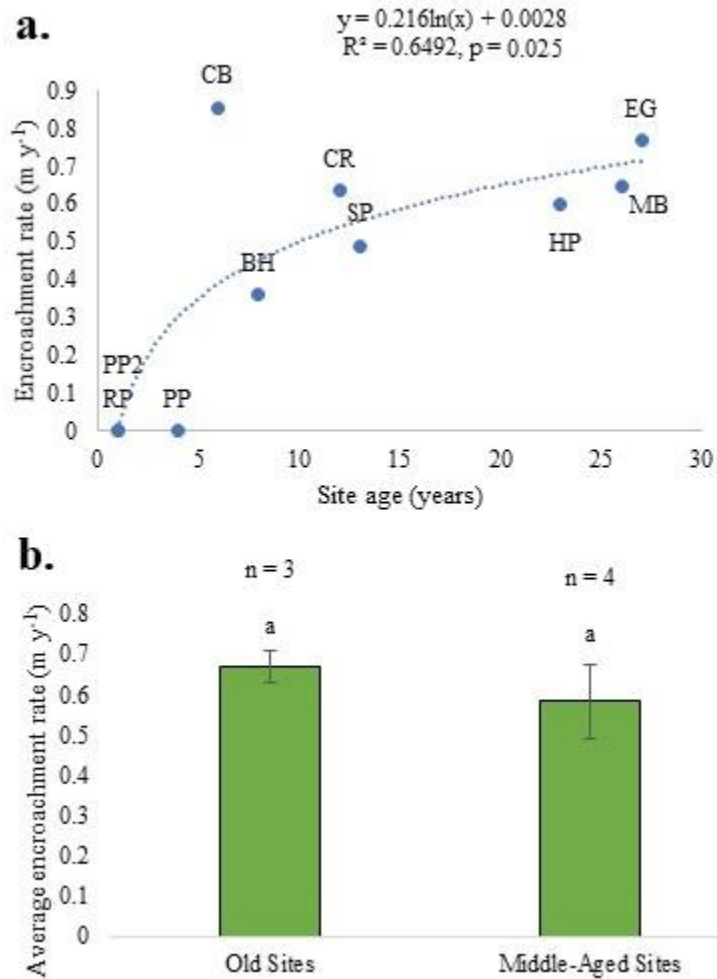


Figure 3. Encroachment rate comparison. a) Site age (years) compared to encroachment rate (m y^{-1}). The dotted blue line signifies a significant, positive logarithmic trend; b) Average encroachment rate (m y^{-1}) compared between old and middle-aged sites. The error bars represent \pm standard error (SE). No difference was observed between the two groups.

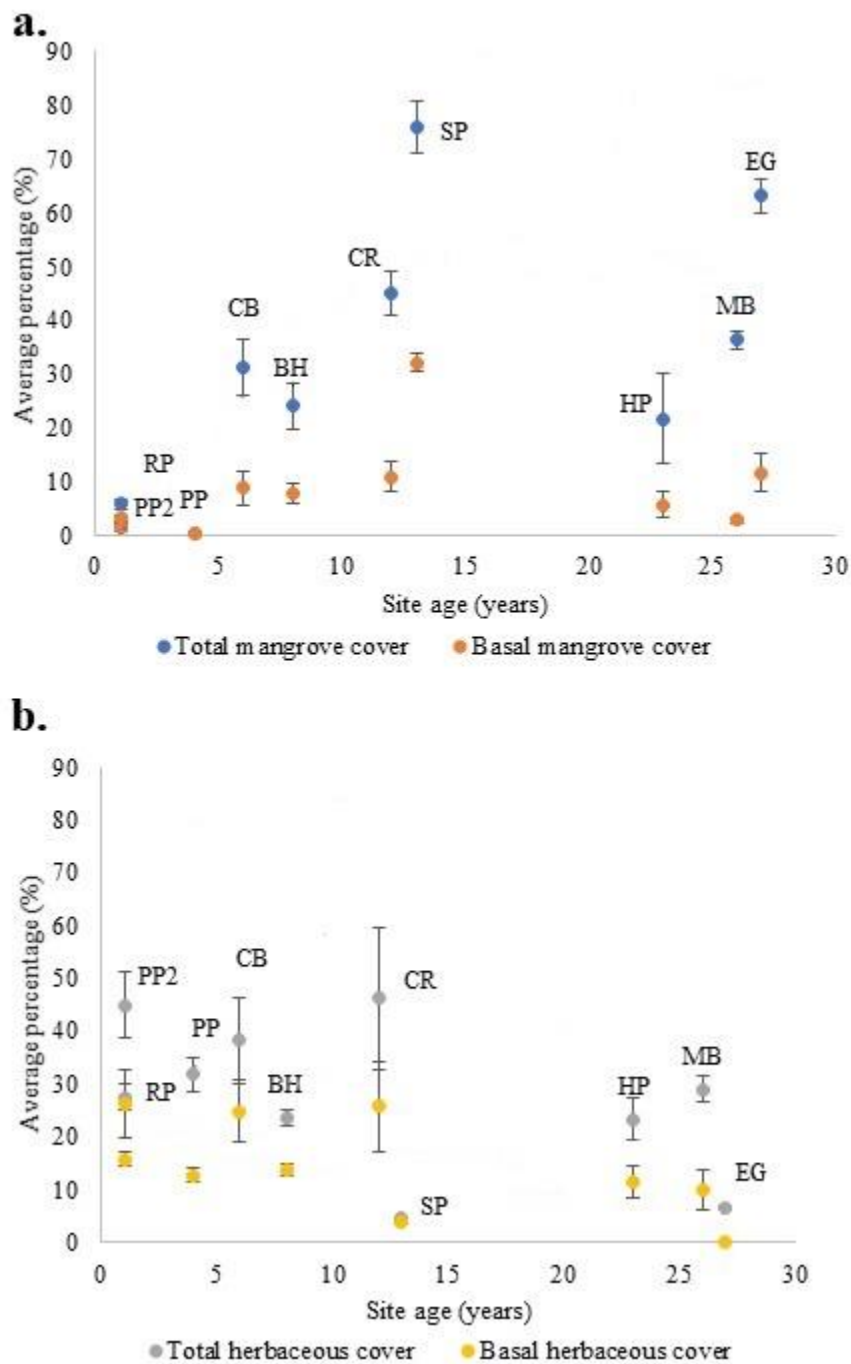


Figure 4. Vegetative percent cover compared to site age. a) Average total and basal mangrove percent cover compared to site age. Error bars represent \pm SE across six plots per site, and the dotted line illustrates a negative quadratic trend; b) Average total and basal herbaceous (non-mangrove) percent cover compared to site age. Error bars represent \pm SE across the six plots.

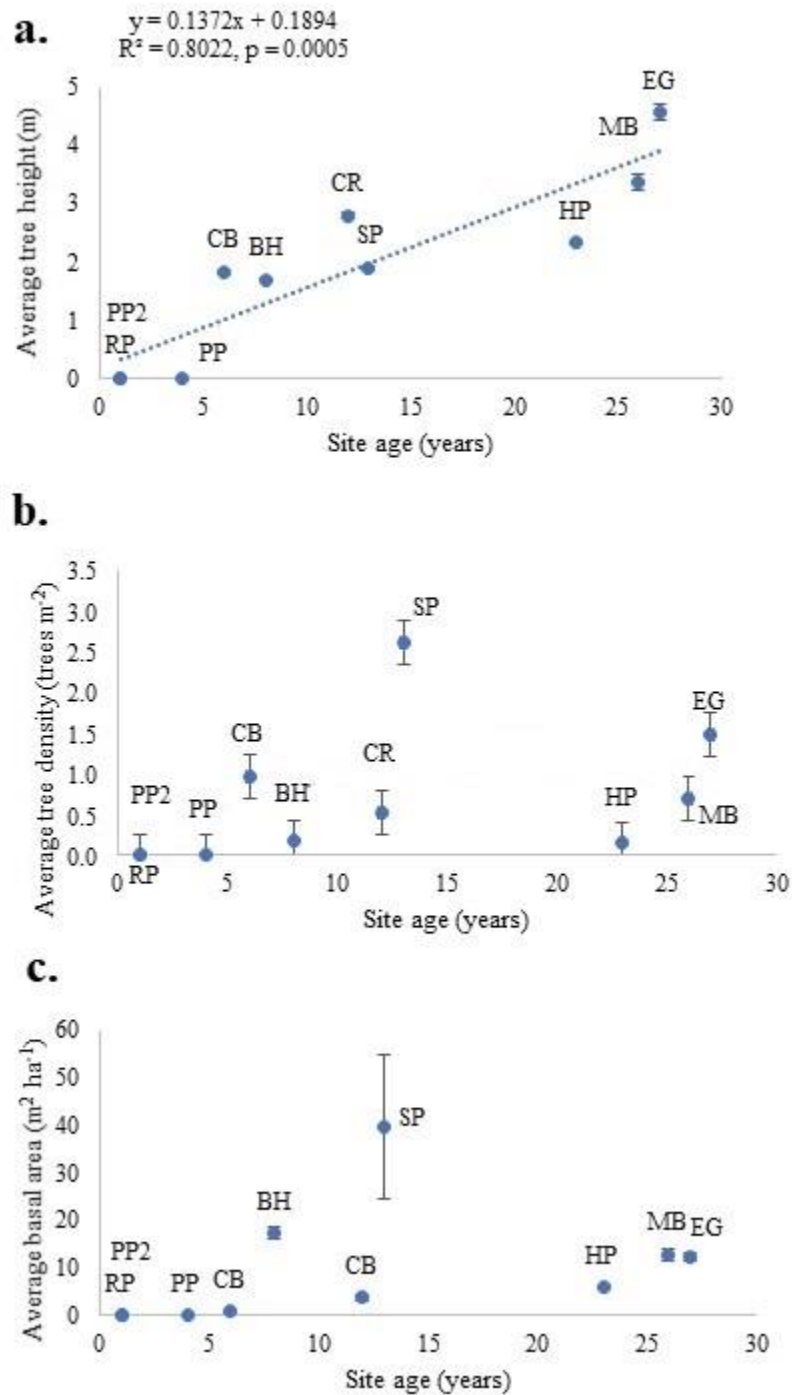


Figure 5. Comparison of tree characteristics. a) Average tree height (m) compared to site age (years). The dotted line illustrates a positive linear relationship; b) Average tree density (trees m⁻²) compared to site age (years). The dotted line represents a negative quadratic relationship; c) Average tree basal area (m² ha⁻¹) compared to site age (years). Error bars signify \pm SE across six plots per site on all graphs.

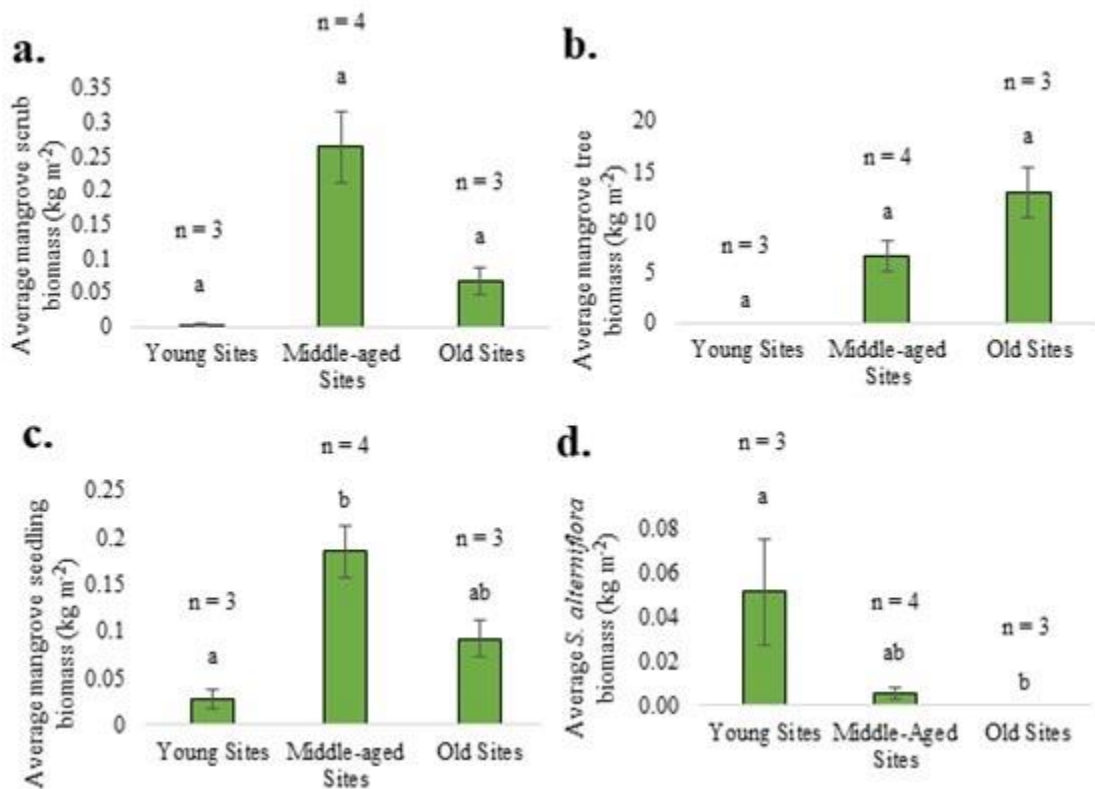


Figure 6. Biomass comparison amongst young, middle-aged, and old sites. a) Average mangrove scrub biomass (kg m⁻²); b) Average mangrove tree biomass (kg m⁻²); c) Average mangrove seedling biomass (kg m⁻²); d) Average *S. alterniflora* biomass (kg m⁻²) across the age classes. Error bars show ± SE across the sites within each age class. Letters denote statistically significant differences (or lack thereof).

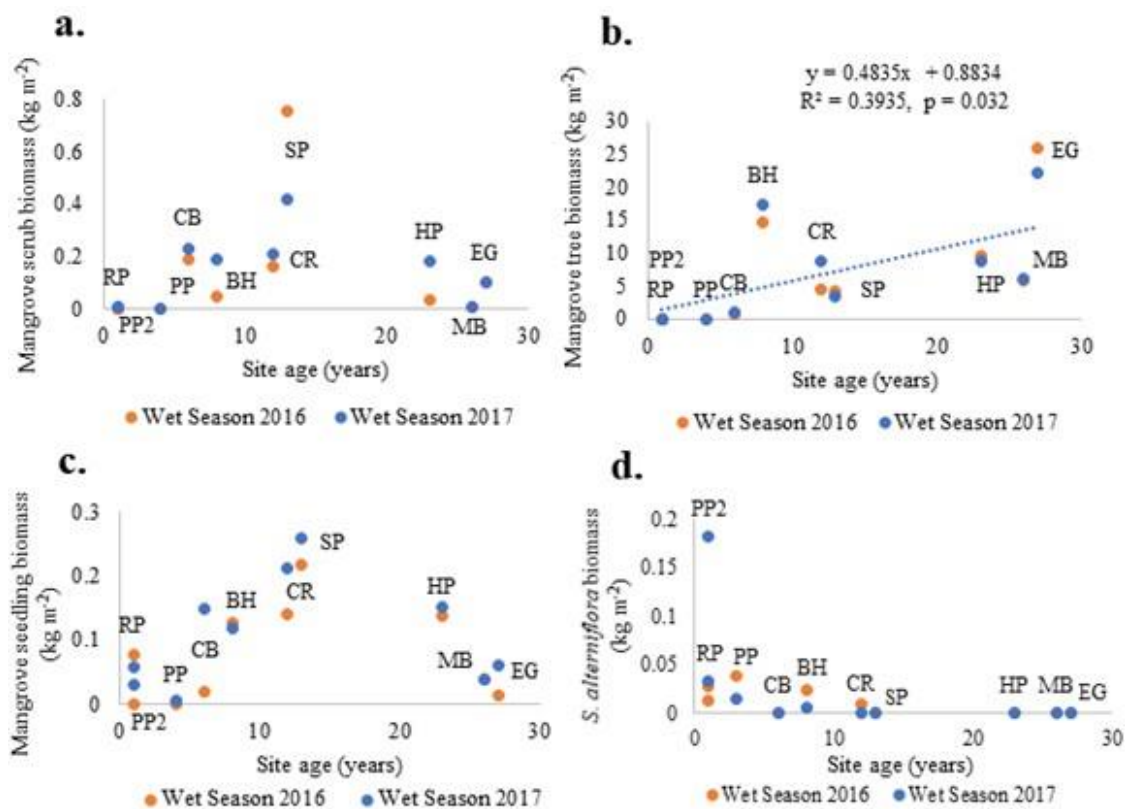


Figure 7. Comparison of vegetative biomass to site age. a) Mangrove scrub biomass (kg m⁻²), b) mangrove tree biomass (kg m⁻²), c) mangrove seedling biomass (kg m⁻²), and d) *S. alterniflora* biomass (kg m⁻²) in 2016 and 2017 compared to site age (years). The dotted line in b) illustrates a significant, positive linear relationship.

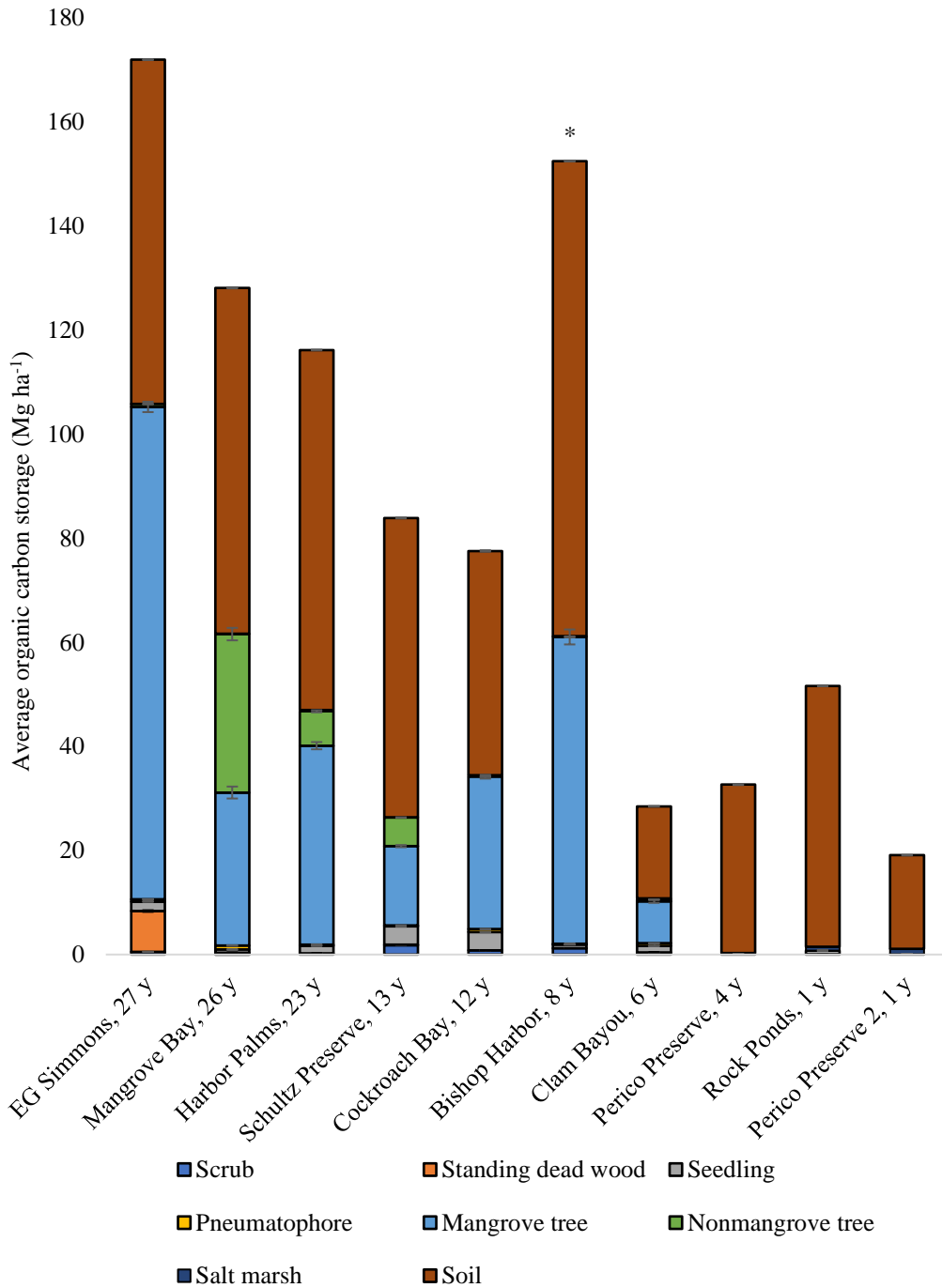


Figure 8. Total organic carbon (OC) storage (Mg ha^{-1}) across the ten restoration sites. Error bars represent \pm SE across the six plots. Ages of the plots displayed in years (y) on the x-axis. The asterisk (*) above Bishop Harbor denotes that this site had high clay content, leading to an erroneously large estimation of organic carbon stocks.

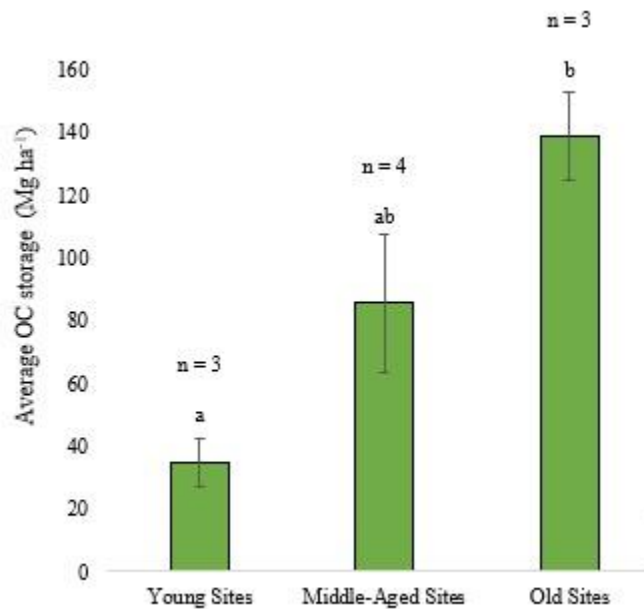


Figure 9. Organic carbon (OC) storage (Mg ha⁻¹) across young, middle-aged, and old restoration sites. Error bars signify \pm SE across the sites in each age category. A difference between biomass at young and old aged sites is designated by the letters ‘a’ and ‘b,’ while ‘ab’ designates that the biomass at middle-aged sites is not different from the other age groups.

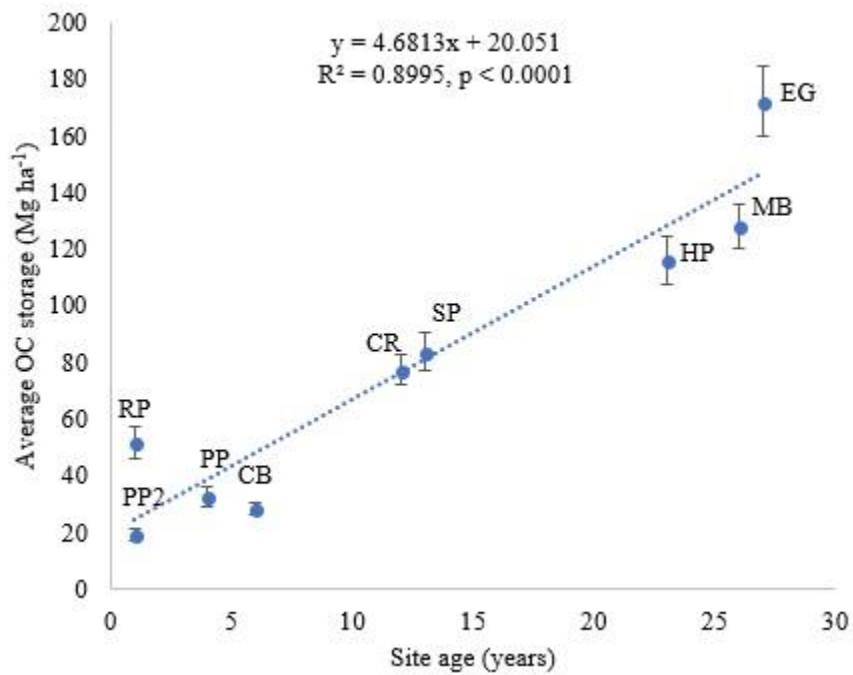


Figure 10. Average organic carbon (OC) storage (Mg ha⁻¹) plotted against site age (years) to calculate the rate of carbon sequestration. The sequestration rate across the 26-year chronosequence was determined by the slope of the trendline, for an average of 4.68 Mg C ha⁻¹ y⁻¹. The error bars indicate \pm SE across the six plots at each site.

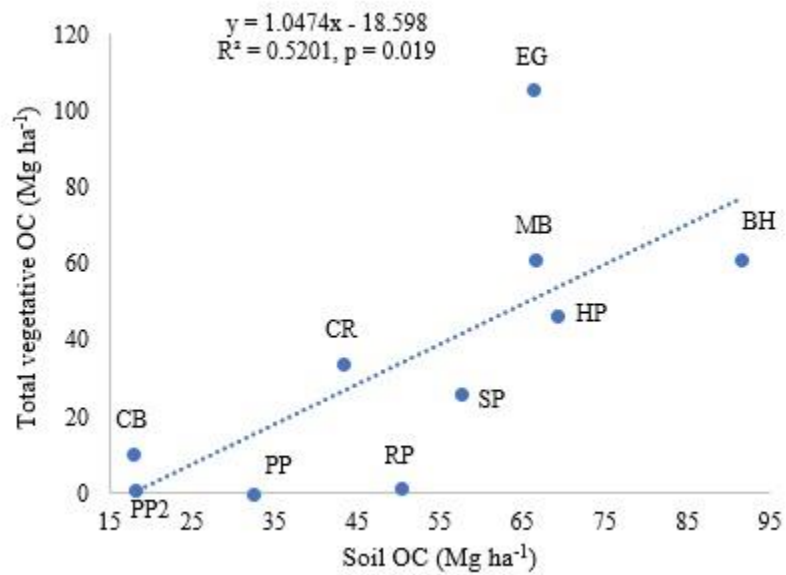


Figure 11. Soil organic carbon (OC) storage (Mg ha⁻¹) compared to total vegetative OC storage across the ten sites. The dotted line illustrates a significant, positive linear relationship.

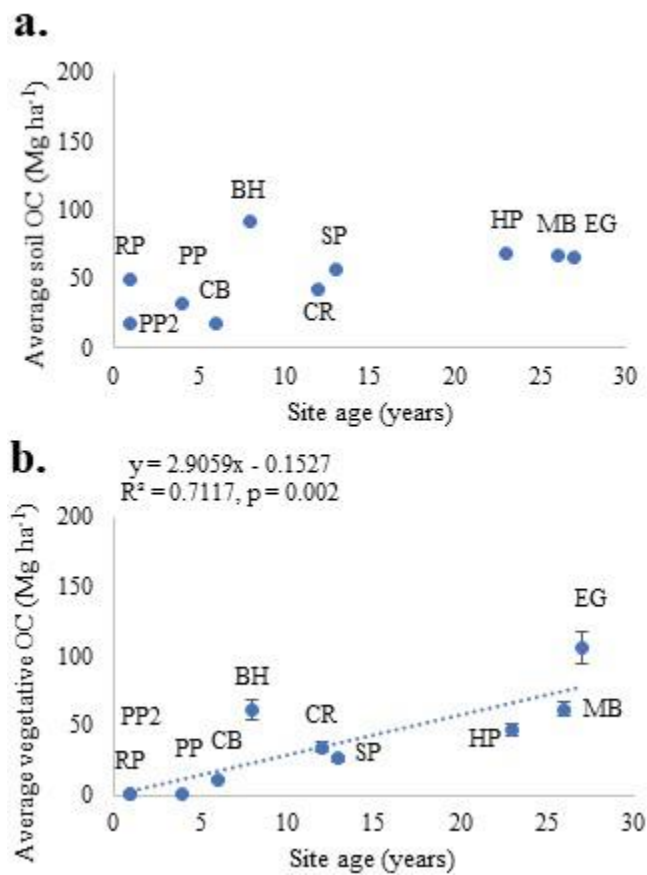


Figure 12. Average a) soil and b) vegetative organic carbon (OC) storage (Mg ha^{-1}) compared to site age. Error bars represent \pm SE across the six plots at each site. The dotted line in b) represents a significant, positive linear trend.

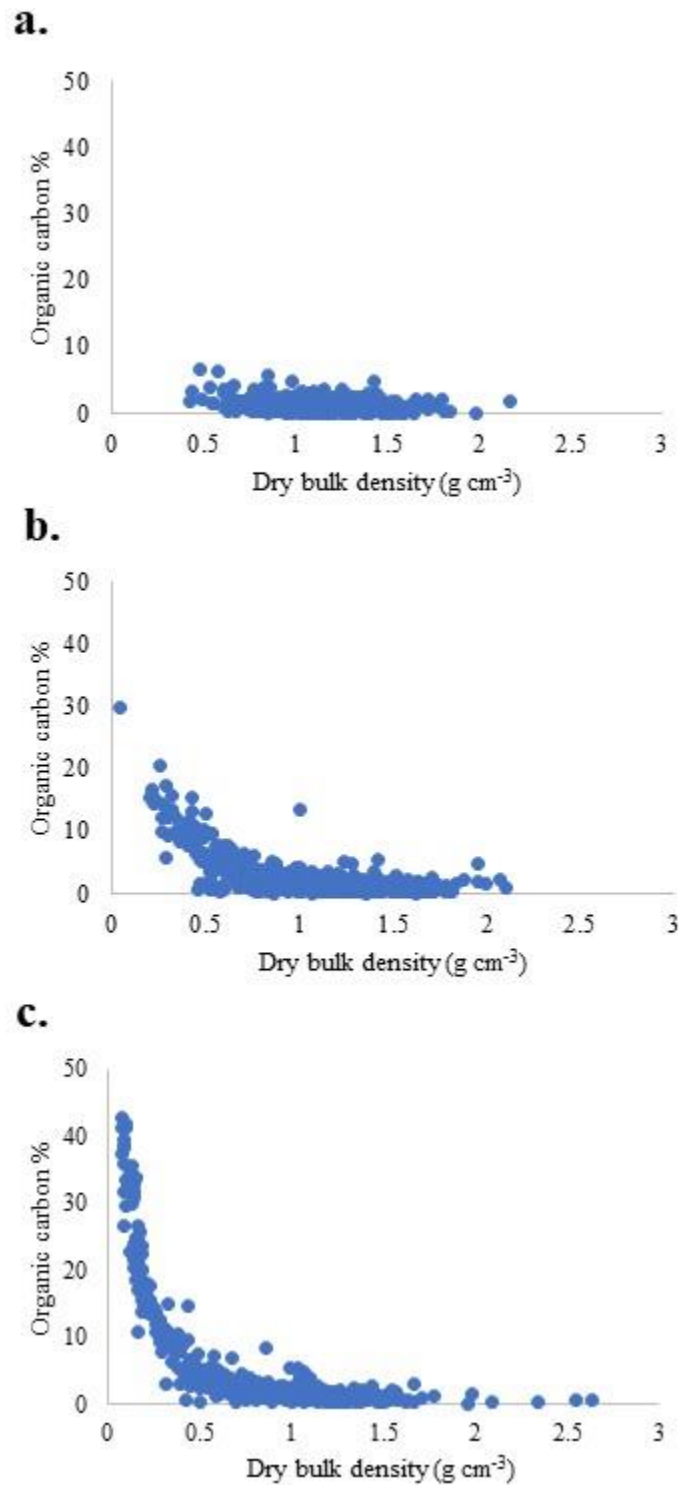


Figure 13. Dry bulk density (DBD) and soil organic carbon (OC%) comparison. a) DBD (g cm⁻³) compared to OC% in 60 soil cores from a) young, b) middle-aged, and c) old restoration sites.

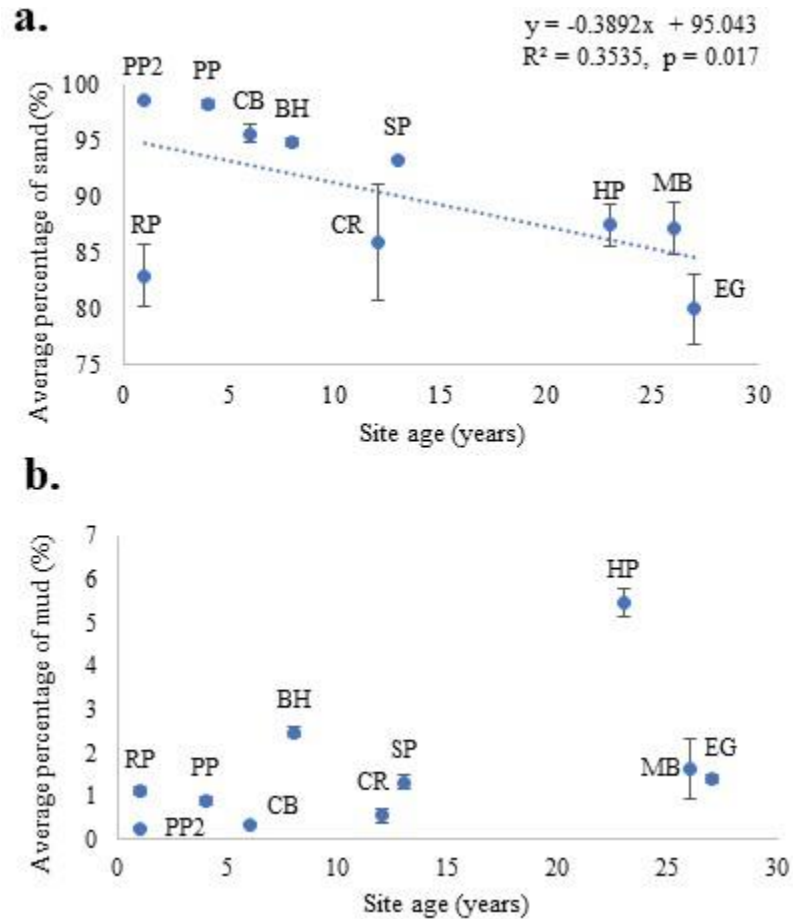


Figure 14. Comparison of site age and average percentage of a) sand and b) mud. Sediment between 0.0625 mm (63 μ m) and 2 mm was considered to be sand, and mud/clay particles were smaller than 0.0625 mm (63 μ m). The dotted line illustrates a significant negative linear trend in a), and the error bars represent \pm SE across six plots per site in both graphs.

REFERENCES

- Abohassan, A., Tewfik, S. F. A., El Wakeel, A. O. 2010. Effect of Thinning on the Above Ground Biomass of (*Conocarpus erectus L.*) Trees in the Western Region of Saudi Arabia. *The Meteorology, Environment and Arid Land Agriculture Journal of King Abdulaziz University* 21: 3-17.
- Adame, M. F., Cherian, S., Reef, R., Stewart-Koster, B. 2017. Mangrove root biomass and the uncertainty of belowground carbon estimations. *Forest Ecology and Management* 403: 52-60.
- Adame, M. F., Santini, N. S., Tovilla, C., Vazquez-Lule, A., Castro, L., Guevara, M., 2015. Carbon stocks and soil sequestration rates of tropical riverine wetlands. *Biogeosciences* 12: 3805-3818.
- Aguaron, E., McPherson, E. G. 2012. Comparison of methods for estimating carbon dioxide storage by Sacramento's urban forest. In: Lal, R., Augustin, B. (Eds.), *Carbon Sequestration in Urban Ecosystems* (43–71). New York: Springer.
- Alongi, D. M. 2014. Carbon Cycling and Storage in Mangrove Forests. *Annual Reviews of Marine Science* 6: 195-219.
- Appolone, E. L. 2000. Organic matter distribution and turnover along a gradient from forest to tidal creek. Master's Thesis, East Carolina University. 161 p.
- Barillé-Boyer, A. L., Barillé, L., Massé, H., Razet, D. Héral, M. 2003. Correction for particulate organic matter as estimated by loss on ignition in estuarine ecosystems. *Estuarine, Coastal and Shelf Science* 58: 147-153.
- Bianchi, T. S., Allison, M. A., Zhao, J., Li, X., Comeaux, R. S., Feagin, R. A., Kulawardhana, R. W. 2013. Historical reconstruction of mangrove expansion in the Gulf of Mexico: Linking climate change with carbon sequestration in coastal wetlands. *Estuarine, Coastal and Shelf Science* 119: 7-16.
- Blott S.J., Pye, K. 2001. GRADISTAT: A grain size distribution and statistics package for the analysis of unconsolidated sediments. *Earth Surface Processes and Landforms* 26: 1237-1248.

- Bosire, J. O., Dahdouh-Guebas, F., Walton, M., Crona, B. I., Lewis, R. R., Field, C., Kairo, J. G., Koedam, N. 2008. Functionality of restored mangroves: a review. *Aquatic Botany* 89: 251-259.
- Bouillon, S., Borges, A. V., Castañeda-Moya, E., Diele, K., Dittmar, T., Duke, N. C., Kristensen, E., Lee, S. Y., Marchand, C., Middelburg, J. J., Rivera-Monroy, V. H., Smith III, T. J., and R. R. Twilley. 2008. Mangrove production and carbon sinks: A revision of global budget estimates. *Global Biogeochemical Cycles* 22: GB2013.
- Bouldin, J. 2008. Some problems and solutions in density estimation from bearing tree data: a review and synthesis. *Journal of Biogeography* 35: 2000-2011.
- Bouma, T. J., De Vries, M. B., Low, E., Peralta, G., Tánčzos, I. V., van de Koppel, J., Herman, P. J. 2005. Trade-offs related to ecosystem engineering: A case study on stiffness of emerging macrophytes. *Ecology* 86: 2187-2199.
- Breithaupt, J. L., Smoak, J. M., Smith, T. J. III, Sanders, C. J. 2014. Temporal variability of carbon and nutrient burial, sediment accretion, and mass accumulation over the past century in a carbonate platform mangrove forests of the Florida Everglades. *Journal of Geophysical Research: Biogeosciences* 119: 2032-2048.
- Breithaupt, J. L., Smoak, J. M., Rivera-Monroy, V. H., Castañeda-Moya, E., Moyer, R. P., Simard, M., Sanders, C. J. 2017. Partitioning the relative contributions of organic matter and mineral sediment to accretion rates in carbonate platform mangrove soils. *Marine Geology* 390: 170-180.
- Castañeda-Moya, E., Twilley, R. R., Rivera-Monroy, V. H., Zhang, K., Davis, S. E., Ross, M. 2010. Sediment and nutrient deposition associated with hurricane Wilma in mangroves of the Florida coastal everglades. *Estuaries and Coasts* 33: 45-58.
- Cavanaugh, K. C., Kellner, J. R., Forde, A. J., Gruner, D. S., Parker, J. D., Rodriguez, W., Feller, I. C. 2014. Poleward expansion of mangroves is a threshold response to decreased frequency of extreme cold events. *Proceedings of the National Academy of Sciences* 111(2): 723-727.
- Chen, Z., Muller-Karger, F. E., Hu, C. 2007. Remote sensing of water clarity in Tampa Bay. *Remote Sensing of Environment* 109: 249-259.
- Chmura, G. L., Anisfeld, S. C., Cahoon, D. R., Lynch, J. C. 2003. Global carbon sequestration in tidal, saline wetland soils. *Global Biogeochemical Cycles* 17(22): 1-12.
- Church, J. A., Clark, P. U., Cazenave, A., Gregory, J. M., Jevrejeva, S., Levermann, A., Merrifield, M. A., Milne, G. A., Nerem, R. S., Nunn, P. D., Payne, A. J., Pfeffer, W. T., Stammer, D., Unnikrishnan, A. S. 2013. 2013: Sea Level Change. In

- Stocker, T.F., D. Qin, G.-K. Plattner, M. Tignor, S.K. Allen, J. Boschung, A. Nauels, Y. Xia, V. Bex and P.M. Midgley (Eds.), *Climate Change 2013: The Physical Science Basis. Contribution of Working Group I to the Fifth Assessment Report of the Intergovernmental Panel on Climate Change*. Cambridge University Press, Cambridge, United Kingdom and New York, NY, USA.
- Comeaux, R.S., Allison, M. A., Bianchi, T. S. 2012. Mangrove expansion in the Gulf of Mexico with climate change: Implications for wetland health and resistance to rising sea levels. *Estuarine, Coastal and Shelf Science* 96: 81-95.
- Cottam, G., Curtis, J. T. 1956. The use of distance measures in phytosociological sampling. *Ecology* 37:451-460.
- Craft, C. B., Seneca, E. D., Broome, S. W. 1991. Loss on ignition and Kjeldahl digestion for estimating organic-carbon and total nitrogen in estuarine marsh soils: calibration with dry combustion. *Estuaries* 14: 175-179.
- Crossland, C. J., Baird, D., Ducrotoy, J., Lindeboom, H. J. 2005. The Coastal Zone – a Domain of Global Interactions. In C. J. Crossland, H. H. Kremer, H. J. Lindeboom, J. I. Marshall Crossland, M. D. A. Le Tissier (Eds.), *Coastal Fluxes in the Anthropocene* (1-34). Berlin, Germany: Springer.
- Dahdouh-Guebas, F., Koedam, N. 2006. Empirical estimate of the reliability of the use of the Point-Centred Quarter Method (PCQM): Solutions to ambiguous field situations and description of the PCQM+ protocol. *Forest Ecology and Management* 228: 1-18.
- Dahl, T. E., Stedman, S. M. 2013. *Status and trends of wetlands in the coastal watersheds of the Conterminous United States 2004 to 2009*. U.S. Department of the Interior, Fish and Wildlife Service and National Oceanic and Atmospheric Administration, National Marine Fisheries Service. 46 p.
- Darby, F. A., Turner, R. E. 2008. Below- and Aboveground *Spartina alterniflora* Production in a Louisiana Salt Marsh. *Estuaries and Coasts* 31: 223-231.
- DeLaune, R. D., Nyman, J. A., Patrick, W. H., Jr. 1994. Peat collapse, ponding and wetland loss in a rapidly submerging coastal marsh. *Journal of Coastal Research* 10(4): 1021-1030.
- DeLaune, R. D., White, J. R. 2012. Will coastal wetlands continue to sequester carbon in response to an increase in global sea level?: a case study of the rapidly subsiding Mississippi river deltaic plain. *Climatic Change* 110: 297-314.
- Donato, D. C., Kauffman, J. B., Murdiyarso, D., Kurnianto, S., Stidham, M., Kanninen, M. 2011. Mangroves among the most carbon-rich forests in the tropics. *Nature Geoscience* 4: 293-297.

- Doughty, C. L., Langley, J. A., Walker, W. S., Feller, I. C., Schaub, R., Chapman, S. K. 2015. Mangrove range expansion rapidly increases coastal wetland carbon storage. *Estuaries and Coasts* 39: 385-396.
- Duarte, C. M., Conley, D. J., Carstensen, J., Sánchez-Camacho, M. 2009. Return to *Neverland*: Shifting baselines affect eutrophication restoration targets. *Estuaries and Coasts* 32(1): 29-36.
- Edwards, K. R., Proffitt, C. E. 2003. Comparison of wetland structural characteristics between created and natural salt marshes in southwest Louisiana, USA. *Wetlands* 23(2): 344-356.
- Ellison, A. M., Farnsworth, E. J. 1997. Simulated sea level change alters anatomy, physiology, growth, and reproduction of red mangrove (*Rhizophora mangle*). *Oecologia* 112: 435-446.
- Ewe, S. M. L., Gaiser, E. E., Childers, D. L., Iwaniec, D., Rivera-Monroy, V. H., Twilley, R. R. 2006. Spatial and temporal patterns of aboveground net primary productivity (ANPP) along two freshwater-estuarine transects in the Florida Coastal Everglades. *Hydrobiologia* 569: 459-474.
- Feller, I. C., Dangremond, E. M., Devlin, D. J., Lovelock, C. E., Proffitt, C. E., Rodriguez, W. 2015. Nutrient enrichment intensifies hurricane damage and prolongs recovery in mangrove ecosystems in the Indian River Lagoon. *Ecology* 96: 2960-2972.
- Feller, I. C., Sitnik, M. (Eds.). 1996. *Mangrove Ecology: A Manual for a Field Course*. Smithsonian Institution.
- Friess, D. A., Krauss, K. W., Horstman, E. M., Balke, T., Bouma, T. J., Galli, D., Webb, E. L. 2012. Are all intertidal wetlands naturally created equal? Bottlenecks, thresholds and knowledge gaps to mangrove and saltmarsh ecosystems. *Biological Reviews* 87: 346-366.
- Fromard, F., Puig, H., Mougin, E., Marty, G., Betoulle, J. L., Cadamuro, L. 1998. Structure, above-ground biomass and dynamics of mangrove ecosystems: new data from French Guiana. *Oecologia* 115:39-53.
- Gardner, R. C., Fox, J. 2013. The Legal Status of Environmental Credit Stacking. *Ecology Law Quarterly* 40: 713-758.
- Glick, P., Clough, J. 2006. *An Unfavorable Tide: Global Warming, Coastal Habitats, and Sportfishing in Florida*. National Wildlife Federation and Florida Wildlife Federation. 56 p.

- Gonneea, M. E. 2016. Tampa Bay carbon burial rates across mangrove and salt marsh ecosystems. In Sheehan, L., Crooks, S (Eds.), *Tampa Bay Blue Carbon Assessment: Summary of Findings*. TBEP Technical Report #07-16. (App. D, 1-50). https://www.tbep.tech.org/TBEP_TECH_PUBS/2016/TBEP_07_16_Tampa-Bay-Blue-Carbon-Assessment-Report-FINAL_June16-2016.pdf. Accessed 21 May 2018.
- GATECC (Governor's Action Team on Energy and Climate Change). 2008. Florida's Energy and Climate Change Action Plan, Center for Climate Strategies, Tallahassee, FL. 124 p. http://www.cakex.org/sites/default/files/documents/Florida%E2%80%99s%20Action%20Plan%20on%20Energy%20and%20Climate%20Change_0.pdf. Accessed 23 Feb. 2018.
- Greening, H., Janicki, A., Sherwood, E. T., Pribble, R., Johansson, J. O. R. 2014. Ecosystem responses to long-term nutrient management in an urban estuary: Tampa Bay, Florida, USA. *Estuarine, Coastal and Shelf Science* 151: A1-A16.
- Guo, H., Zhang, Y., Lan, Z., Pennings, S. C. 2013. Biotic interactions mediate the expansion of black mangrove (*Avicennia germinans*) into salt marshes under climate change. *Global Change Biology* 19: 2765-2774.
- Holland, N., Hoppe, M. K., Cross, L. 2006. *Implement the Tampa Bay Master Plan for Habitat Restoration and Protection. Charting the Course: The Comprehensive Conservation and Management Plan for Tampa Bay*, Tampa Bay Estuary Program. 151 p.
- Hopkinson, C. S., Cai, W., Hu, X. 2012. Carbon sequestration in wetland dominated coastal systems – a global sink of rapidly diminishing magnitude. *Current Opinion in Environmental Sustainability* 4: 1-9.
- Howard, J., Hoyt, S., Isensee, K, Pidgeon, E., Telszewski, M. (Eds). 2014. *Coastal Blue Carbon: Methods for assessing carbon stocks and emissions factors in mangroves, tidal salt marshes, and seagrass meadows*. Conservation International, Intergovernmental Oceanographic Commission of UNESCO, International Union for Conservation of Nature. Arlington, Virginia, USA.
- Kangas, P.C., Lugo, A.E. 1990. The distribution of mangroves and saltmarsh in Florida. *Tropical Ecology* 31(1): 32–39.
- Kauffman, J. B., Donato, D.C. 2012. *Protocols for the measurement, monitoring and reporting of structure, biomass and carbon stocks in mangrove forests*. Working Paper 86. CIFOR, Bogor, Indonesia. 50 p.

- Kelleway, J. J., Cavanaugh, K., Rogers, K., Feller, I. C., Ens, E., Doughty, C., Saintilan, N. 2017. Review of the ecosystem service implications of mangrove encroachment into salt marshes. *Global Change Biology* 23(10): 3967-3983.
- Kelleway, J. J., Saintilan, N., Macreadie, P. I., Skilbeck, C. G., Zawadzki, A., Ralph, P. J., 2016. Seventy years of continuous encroachment substantially increases 'blue carbon' capacity as mangroves replace intertidal salt marshes. *Global Change Biology* 22: 1097-1109.
- Kennedy, H., Alongi, D. M., Karim, A. 2013. Coastal Wetlands. In N. M. Bortalba, G. K. Hiebaum (Eds.), *2006 IPCC Guidelines for National Greenhouse Gas Inventories: Wetlands* (6-43).
- Kennish, M. J. 2001. Coastal Salt Marsh Systems in the U.S.: A Review of Anthropogenic Impacts. *Journal of Coastal Research* 17(3): 731-748.
- Khan, M. N. I., Hijbeek, R., Berger, U., Koedam, N., Grueters, U., Islam, S. M. Z., Hasan, M. A., Dahdouh-Guebas, F. 2016. An Evaluation of the Plant Density Estimator the Point-Centred Quarter Method (PCQM) Using Monte Carlo Simulation. *PLoS One* 11(6): 1-18.
- Khan, M.N.I., Suwa, R., Hagihara, A. 2009. Biomass and aboveground net primary production in a subtropical mangrove stand of *Kandelia obovata* (S., L.) Yong at Manko Wetland, Okinawa. *Japan Wetlands Ecology and Management* 17: 585-599.
- Kirwan, M. L., Megonigal, J. P. 2013. Tidal wetland stability in the face of human impacts and sea-level-rise. *Nature* 504: 53-60.
- Krauss, K. W., Cormier, N., Osland, M. J., Kirwan, M. L., Stagg, C. L., Nestlerods, J. A., Russell, M. J., From, A. S., Spivak, A. C., Dantin, D., Harvey, J. E., Almario, A. E. 2017. Created mangrove wetlands store belowground carbon and surface elevation change enables them to adjust to sea-level rise. *Nature Scientific Reports* 7(1): 1-11.
- Lewis, R. R. III, Clark, P. A., Fehring, W. K., Greening, H. S., Johansson, R. O., Paul, R. T. 1998. The Rehabilitation of the Tampa Bay Estuary, Florida, USA, as an Example of Successful Integrated Coastal Management. *Marine Pollution Bulletin* 37(8-12): 468-473.
- Lewis R.R. III, Estevez, E.D. 1988. *The ecology of Tampa Bay, Florida: an estuarine profile*. Fish and Wildlife Service - U.S. Department of the Interior. Biological report 85(7.18). 132 p.

- Lewis, R. R. III, Robison, D. 1995. *Setting priorities for Tampa Bay habitat protection and restoration: restoring the balance*. Prepared by Lewis Environmental Services, Inc. and Coastal Environmental, Inc. 241 p.
- Lewis, R. R. III. 2005. Ecological engineering for successful management and restoration of mangrove forests. *Ecological Engineering* 24: 403-418.
- Linacre, N., Kossoy, A., Ambrosi, P. 2011. *States and trends of the carbon market 2011*. The World Bank 2011 Report, Washington, DC. 80 p.
- López-Portillo, J., Ezcurra, E. 1989. Zonation in Mangrove and Salt Marsh Vegetation at Laguna de Mecoacán, México. *Biotropica* 21(2): 107-114.
- Mack, S. K., Yankel, C., Lane, R. R., Day, J. W., Kempka, D., Mack, J. S., Hardee, E., LeBlanc, C. 2014. *Carbon Market Opportunities for Louisiana's Coastal Wetlands*. *Tierra Resources*, prepared for Entergy Corporation's Environmental Initiatives Fund 2014. <https://climatetrust.org/wp-content/uploads/2015/03/Carbon-Market-Opportunities-for-Louisiana%E2%80%99s-Coastal-Wetlands-150305-CS-FNL.pdf>. Accessed 13 May 2018.
- Marchio, D. A., Jr., Savarese, M., Bovard, B., Mitsch, W. J. 2016. Carbon sequestration and sedimentation in mangrove swamps influenced by hydrogeomorphic conditions and urbanization in Southwest Florida. *Forests* 7(6): 116.
- Mazumder, D., Saintilan, N., Williams, R. J. 2009. Zooplankton inputs and outputs in the saltmarsh at Towra Point, Australia. *Wetlands Ecology and Management* 17: 225-230.
- McLeod, E., Chmura, G. L., Bouillon, S., Salm, R., Björk, M., Duarte, C. M., Lovelock, C. E., Schlesinger, W. H., Silliman, B. R. 2011. A blueprint for blue carbon: toward an improved understanding of the role of vegetated coastal habitats in sequestering CO₂. *Frontiers in Ecology and the Environment* 9(10): 552-560.
- Michener, J. W., Blood, E. R., Bildstein, K. L., Brinson, M. M., Gardner, L. R. 1997. Climate change, hurricanes and tropical storms, and rising sea level in coastal wetlands. *Ecological Applications* 7(3): 770-801.
- Mitchell, K. 2015. Quantitative analysis by the point-centered quarter method. 56 p. <https://arxiv.org/pdf/1010.3303.pdf>. Accessed 20 February 2018.
- Moore, G. E., Burdick, D. M., Peter, C. R., Keirstead, D. R. 2011. Mapping Soil Pore Water Salinity of Tidal Marsh Habitats Using Electromagnetic Induction in Great Bay Estuary, USA. *Wetlands* 31(2): 309-318.

- Morris, J., Barber, D. C., Callaway, J. C., Chambers, R., Hagen, S. C., Hopkinson, C. S., Johnson, B. J., Megonigal, P., Neubauer, S. C., Troxler, T., Wigand, C. 2016. Contributions of organic and inorganic matter to sediment volume and accretion in tidal wetlands at steady state. *Earth's Future* 4: 1-11.
- Morisita, M. 1957. A new method for the estimation of density by the spacing method, applicable to non-randomly distributed populations. *Physiology and Ecology – Kyoto 7*: 134-144 (in Japanese). [English translation (1960) Division of Range Management and Wildlife Habitat Research, US Forest Service, M-5123].
- Murphy, S., Voulgaris, G. 2007. Identifying the role of tides, rainfall and seasonality in marsh sedimentation using long-term suspended sediment concentration data. *Marine Geology* 227: 31-50.
- Nellemann, C., Corcoran, E., Duarte, C. M., Valdés, L., De Young, C., Fonseca, L., Grimsditch, G. (Eds). 2009. *Blue Carbon: The Role of Healthy Oceans in Binding Carbon*. United Nations Environment Programme, GRID-Arendal.
- NERRS SWMP (National Estuarine Research Reserve System Wide Monitoring Program). Vegetation Monitoring Protocol. 2013. *Long-term monitoring of estuarine vegetation communities*. National Estuarine Research Reserve System Technical Report. 36 p.
- Nyman, J. A., Walters, R. J., Delaune, R. D., Patrick, W. H., 2006. Marsh vertical accretion via vegetative growth. *Estuarine and Coastal Shelf Science* 69: 370-380.
- Osland, M. J., Enwright, N., Day, R. H., Doyle, T. W. 2013. Winter climate change and coastal wetland foundation species: salt marshes vs. mangrove forests in the southeastern United States. *Global Change Biology* 19(5): 1482-1494.
- Osland, M. J., Spivak, A. C., Nestlerode, J. A., Lessmann, J. M., Almario, A. E., Heitmuller, P. T., Russell, M. J., Krauss, K. W., Alvarez, F., Dantin, D. D., Harvey, J. E., From, A. S., Cormier, N., Stagg, C. L. 2012. Ecosystem Development after Mangrove Wetland Creation: Plant-Soil Change Across a 20-Year Chronosequence. *Ecosystems* 15: 848-866.
- Pennings, S. C., Grant, B., Bertness, M. D. 2005. Plant zonation in low-latitude salt marshes: Disentangling the roles of flooding, salinity and competition. *Ecology* 93: 159-167.
- Proum, S., Santos, J. H., Lim, L. H., Marshall, D. J. 2018. Tidal and seasonal variation in carbonate chemistry, pH and salinity for a mineral-acidified tropical estuarine system. *Regional Studies in Marine Science* 17: 17-27.

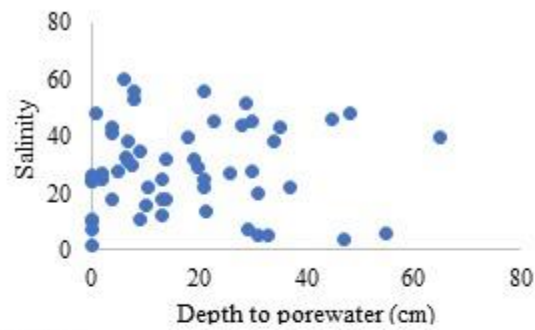
- Raabe, E. A., Roy, L. C., McIvor, C. C. 2012. Tampa Bay Coastal Wetlands: Nineteenth to Twentieth Century Tidal Marsh-to-Mangrove Conversion. *Estuaries and Coasts* 35: 1145-1162.
- Radabaugh, K. R., Moyer, R. P., Chappel, A. R., Powell, C. E., Bociu, I., Clark, B. C., Smoak, J. M. 2018. Coastal blue carbon assessment of mangroves, salt marshes, and salt barrens in Tampa Bay, Florida, USA. *Estuaries and Coasts* 41(5): 1496-1510.
- Radabaugh, K. R., Powell, C. E., Bociu, I., Clark, B. C., Moyer, R. P. 2017. Plant size metrics and organic carbon content of Florida salt marsh vegetation. *Wetlands Ecology and Management* 24(6): 3-15.
- Robison, D., Krebs, A., Fouts, J. 2010. *Tampa Bay Estuary Program Habitat Master Plan Update*. PBS&J International, Inc., Tampa, Florida. 153 p.
- Robison, D., Sheehan, L., Quinton, B., Tomasko, D., Crooks, S. Management of Tampa Bay blue carbon habitats in response to sea-level rise. 2015. In Burke, M. (Ed.), *BASIS 6 Proceedings: Navigating Changing Tides* (242-258). St. Petersburg, FL.
- Ross, M. S., Ruiz, P. L., Telesnicki, G. J., Meeder, J. F. 2001. Estimating above-ground biomass and production in mangrove communities of Biscayne National Park, Florida (U.S.A.). *Wetlands Ecology and Management* 9: 27-37.
- Schmidt, N., Luther, M. E. 2002. ENSO Impacts on Salinity in Tampa Bay, Florida. *Estuaries* 25(5): 976-984.
- Shafer, D. J., Roberts, T. H. 2008. Long-term development of tidal mitigation wetlands in Florida. *Wetlands Ecology and Management* 16: 23-31.
- Shaffer, G. P., Day Jr, J. W., Mack, S., Kemp, G. P., Van Heerden, I., Poirrier, M. A., Westphal, K. A., Fitzgerald, D., Milanese, A., Morris, C. A., Bea, R., Penland, P. S. 2009. The MRGO navigation project: A massive human-induced environmental, economic, and storm disaster. *Journal of Coastal Research* 54: 206-224.
- Sherwood, E. T., Greening, H. S. 2014. Potential Impacts and Management Implications of Climate Change on Tampa Bay Estuary Critical Coastal Habitats. *Environmental Management* 53: 401-415.
- Siikamäki, J., Sanchirico, J. N., Jardine, S. L. 2012. Global economic potential for reducing carbon dioxide emission from mangrove loss. *Proceedings of the National Academy of Sciences* 109(36): 14369-14374.

- Smee, D. L., Sanchez, J. A., Diskin, M., Trettin, C. 2017. Mangrove expansion into salt marshes alters associated faunal communities. *Estuarine, Coastal and Shelf Science* 187: 306-313.
- Smith, T. J. III, Anderson, G. H., Balentine, K., Tiling, G., Ward, G. A., Whelan, K. R. T. 2009. Cumulative impacts of hurricanes on Florida mangrove ecosystems: sediment deposition, storm surges and vegetation. *Wetlands* 29: 24-34.
- Smith, T. J. III, Tiling, G., Leasure, P. S. 2007. Restoring coastal wetlands that were ditched for mosquito control: A preliminary assessment of hydro-leveling as a restoration technique. *Journal of Coastal Conservation* 11: 67-74.
- Smith, T. J. III, Whelan, K. R. T. 2006. Development of allometric relations for three mangrove species in South Florida for use in the Greater Everglades Ecosystem restoration. *Wetlands Ecology and Management* 14: 409-419.
- Snedden, G. A., Steyer, G. D. 2013. Predictive occurrence models for coastal wetland plant communities: Delineating hydrologic response surfaces with multinomial logistic regression. *Estuarine, Coastal and Shelf Science* 118: 11-23.
- SER (Society for Ecological Restoration). 2002. SER International Science and Policy Working Group. The SER Primer on Ecological Restoration. <https://www.ser.org/content/ecological-restoration-primer.asp>. Accessed 27 June 2018.
- SFRCCC (Southeast Florida Regional Climate Change Compact) Technical Ad hoc Work Group, April 2011. *A unified sea level rise projection for Southeast Florida*. A document prepared for the Southeast Florida Regional Climate Change Compact Steering Committee. <https://southeastfloridaclimatecompact.files.wordpress.com/2014/05/sea-level-rise.pdf>. 27 p.
- Stevens, K. A., DeAngelo, G., Brice, S. 2011. Comparative study of selected greenhouse gas offset protocols. *International Journal of Climate Change Strategies and Management* 3(2): 118-139.
- Stevens, P. W., Fox, S. L., Montague, C. L. 2006. The interplay between mangroves and saltmarshes at the transition between temperate and subtropical climate in Florida. *Wetlands Ecology and Management* 14: 435-444.
- Stout, J. P. 1984. *The ecology of irregularly flooded salt marshes of the northeastern Gulf of Mexico: a community profile*. U. S. Fish and Wildlife Service Biological Reports 85(7.1). 98 p.
- Sutton-Grier, A. E., Moore, A. 2016. Leveraging Carbon Services of Coastal Ecosystems for Habitat Protection and Restoration. *Coastal Management* 44(3): 259-277.

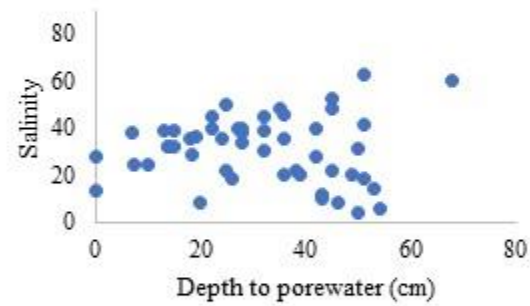
- SWFWMD (Southwest Florida Water Management District) 2012. Land use/land cover 2011 GIS Shapefile Database.
http://data.swfwmd.opendata.arcgis.com/datasets/f325a3417c92444d9cba838154d6fa0d_11. Accessed 23 Feb. 2018.
- TBEP (Tampa Bay Estuary Program). 2017. *Charting the Course: The Comprehensive Conservation and Management Plan for Tampa Bay*. 158 p.
http://www.tampabay.wateratlas.usf.edu/upload/documents/192_tbep_ccmp_2017-web.pdf. Accessed 25 May 2018.
- United States Census Bureau. 2016. Cumulative Estimates of Resident Population Change and Rankings: April 1, 2010 to July 1, 2016.
<http://factfinder.census.gov/faces/tableservices/jsf/pages/productview.xhtml?src=bkmk>. Accessed 20 Feb. 2018.
- Vázquez-González, C., Moreno-Casasola, P., Hernández, M. E., Campos, A., Espejel, I., Fermán-Almada, J. L. 2017. Mangrove and Freshwater Wetland Conservation Through Carbon Offsets: A Cost-Benefit Analysis for Establishing Environmental Policies. *Environmental Management* 59: 274-290.
- VCS (Verified Carbon Standard). 2015. VM0033: Methodology for Tidal Wetland and Seagrass Restoration, Version 1. Developed by Restore America's Estuaries and Silvestrum, Sectoral scope 14. http://database.v-c-s.org/sites/vcs.benfredaconsulting.com/files/VM0033%20Tidal%20Wetland%20and%20Seagrass%20Restoration%20v1.0%2020%20NOV%202015_0.pdf. Accessed 23 Feb. 2018.
- Villa, J. A., Bernal, B. 2017. Carbon sequestration in wetlands, from science to practice: An overview of the biogeochemical process, measurement methods, and policy framework. *Ecological Engineering* 114: 115-128.
- Wang, P. F., Martin, J., Morrison, G. 1999. Water Quality and Eutrophication in Tampa Bay, Florida. *Estuarine, Coastal, and Shelf Science* 49: 1-20.
- Warde, W., Petranka, J. W. 1981. A correction factor table for missing point-center quarter data. *Ecology* 62(2): 491-494.
- Xian, G., Crane, M., Su, J. 2007. An analysis of urban development and its environmental impact on the Tampa Bay watershed. *Journal of Environmental Management* 85: 965-976.
- Yates, K. K., Greening, H. 2011. An Introduction to Tampa Bay. In K. K. Yates, H. Greening, G. Morrison (Eds.), *Integrating Science and Resource Management in Tampa Bay, Florida* (1-16). Reston, VA: USGS.

Appendix A: Supplemental Abiotic Figures

A1a.



A1b.



A1c.

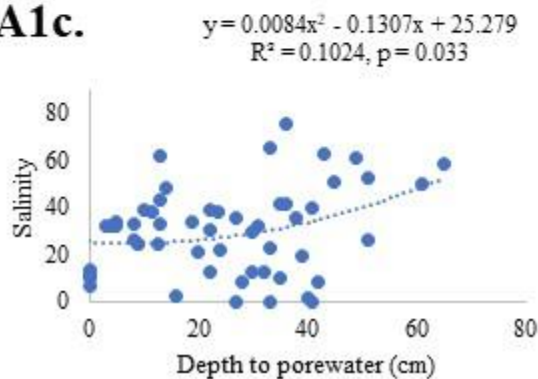


Figure A1. Depth to porewater (cm) compared to salinity in the a) wet season 2016 (June-September), b) dry season 2017 (January-March), and wet season 2017. In c), the dotted line illustrates a positive quadratic relationship.

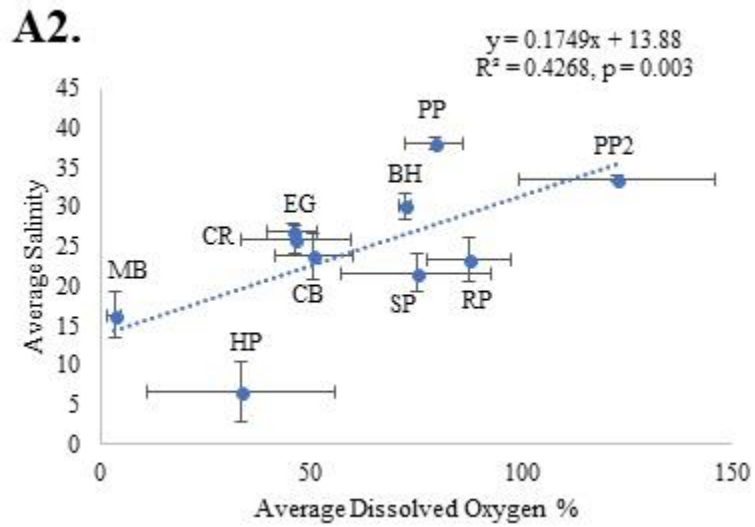


Figure A2. Average open water dissolved oxygen percentage (%) compared to average open water salinity across the ten sites. Error bars signify \pm SE across the three sampling periods. The dotted line illustrates a significant, positive linear relationship.

A3.

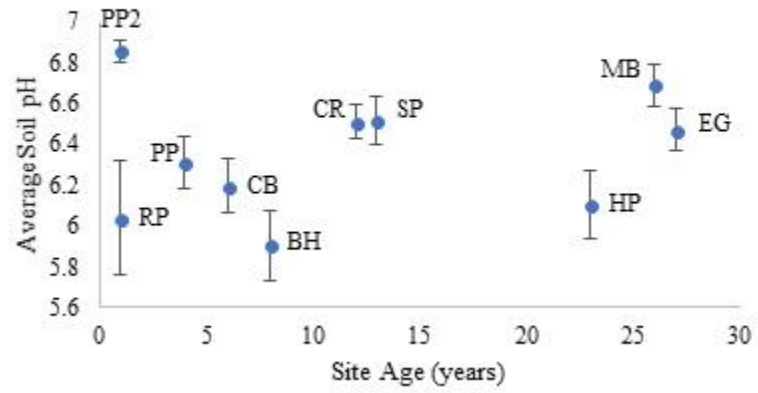


Figure A3. Site age compared to average pH of the top 5-cm of soil. Error bars show \pm SE across the six plots at each site.

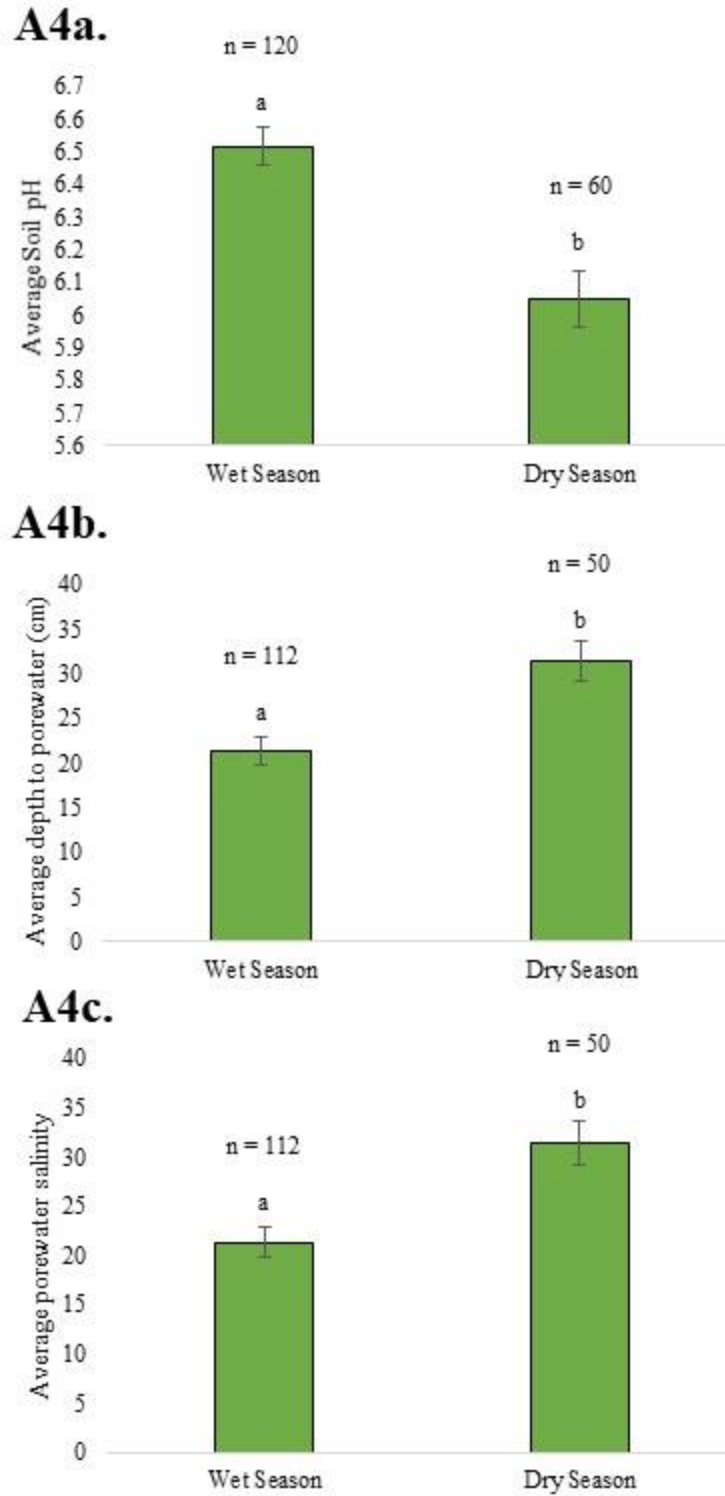


Figure A4. Seasonal comparison of average a) soil pH, b) depth to porewater (cm), and c) porewater salinity. Error bars signify \pm SE across the six plots at each site. Wet season averages were calculated based on data collected in 2016 and 2017. The letters ‘a’ and ‘b’ above the bars indicate that a significant difference exists between the two seasons.

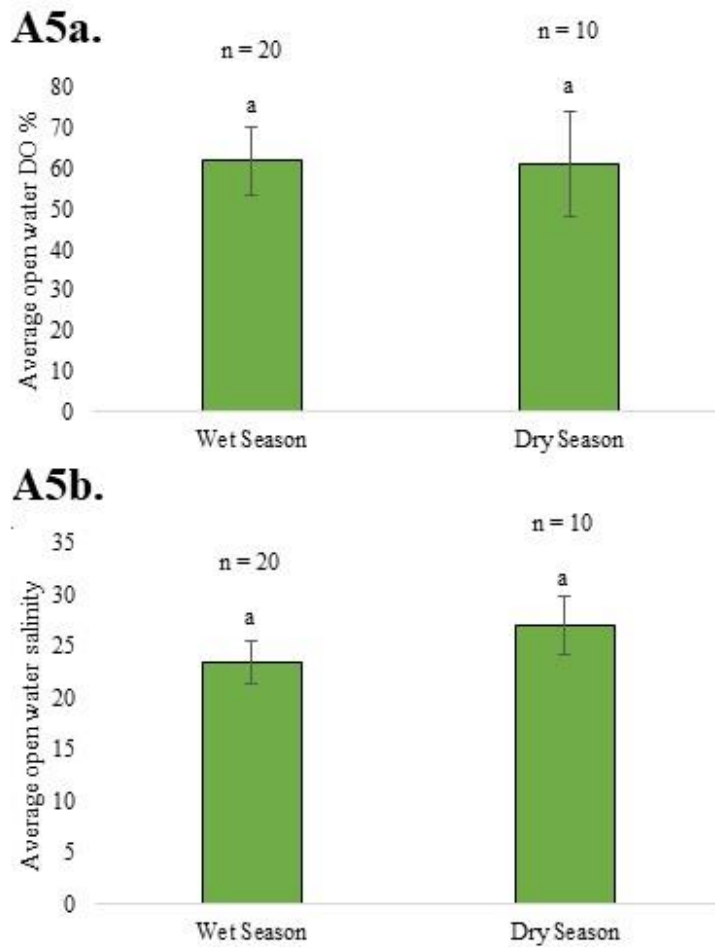


Figure A5. Seasonal comparison of average a) open water dissolved oxygen percentage (DO%) and b) open water salinity. Error bars signify \pm SE across the six plots at each site. Wet season averages were calculated based on data collected in 2016 and 2017. The letter ‘a’ above the bars indicates that no difference exists between the two seasons.

There was not a correlation between depth to porewater and porewater salinity in the wet season 2016 ($r = 0.16676$, $df = 55$, $p = 0.2150$; Fig. A1a), nor in the dry season 2017 ($r = -0.00632$, $df = 48$, $p = 0.9653$; Fig. A1b), but there was a positive correlation between the two variables in the wet season 2017 ($r = 0.28868$, $df = 53$, $p = 0.0326$; Fig. A1c). A comparison between open water DO% and open water salinity yielded a significant positive correlation ($r = 0.52084$, $df = 8$, $p = 0.0032$; Fig. A2). No relationship was detected between site age and soil pH, though ($r = 0.18285$, $df = 8$, $p = 0.6131$). A significant difference was observed between soil pH (*paired t* = -3.49, $df = 59$, $p = 0.0009$; Fig. A4a), depth to porewater (*paired t* = 6.23, $df = 47$, $p < 0.0001$; Fig. A4b), and porewater salinity (*paired t* = 2.37, $df = 47$, $p = 0.0220$; Fig. A4c) in the wet seasons and dry season. Finally, there was not a difference in open water DO% (*paired t* = 0.04, $df = 9$, $p = 0.9671$; Fig. A5a), nor was there a difference in open water salinity (*paired t* = 2.86, $df = 9$, $p = 0.188$; Fig. A5b) in the wet seasons and dry season.

In this study, average pH in the top 5-cm of the soil profile across all sites was 6.5 ± 0.1 in the wet seasons and 6.1 ± 0.2 in the dry season, indicative of seasonal variation, as soils experience prolonged inundation and greater flushing in the wet season. Rainfall provides a source of freshwater, which lowers both the soil salinity and pH (Proum et al. 2018). An excess of rainfall also dilutes estuarine waters via freshwater runoff, which explains the lower open-water salinity in the wet season (App. A) (Murphy and Voulgaris 2006). Further, heightened rainfall leads to a higher mean sea level, resulting in prolonged inundation of marshes, which allows porewater to rise closer to the soil's surface (Murphy and Voulgaris 2006). Salinity and flood duration are critical to the success of restored salt marshes, as shortened or extended inundation can hinder the growth of vegetation (Moore

et al. 2011). Moore et al. (2011) further determined that sites with suitable hydrologic connectivity tend to have lower porewater salinity and thus, more salt marsh growth. In addition to soil pH and open water salinity, other abiotic factors measured in this study that revealed significant seasonal differences were depth to porewater and porewater salinity (App. A).